



## Review

## Viscoelasticity of ECM and cells—origin, measurement and correlation

Zhiqiang Liu, Si Da Ling, Kaini Liang, Yihan Chen, Yudi Niu, Lei Sun, Junyang Li, Yanan Du\*

Department of Biomedical Engineering, School of Medicine, Tsinghua-Peking Center for Life Sciences, Tsinghua University, Beijing 100084, China

## ARTICLE INFO

## Keywords:

Extracellular matrix  
Cell  
Viscoelasticity  
Origin  
Measurement  
Correlation

## ABSTRACT

The extracellular matrix (ECM) and cells are crucial components of natural tissue microenvironments, and they both demonstrate dynamic mechanical properties, particularly viscoelastic behaviors, when exposed to external stress or strain over time. The capacity to modify the mechanical properties of cells and ECM is crucial for gaining insight into the development, physiology, and pathophysiology of living organisms. As an illustration, researchers have developed hydrogels with diverse compositions to mimic the properties of the native ECM and use them as substrates for cell culture. The behavior of cultured cells can be regulated by modifying the viscoelasticity of hydrogels. Moreover, there is widespread interest across disciplines in accurately measuring the mechanical properties of cells and the surrounding ECM, as well as exploring the interactive relationship between these components. Nevertheless, the lack of standardized experimental methods, conditions, and other variables has hindered systematic comparisons and summaries of research findings on ECM and cell viscoelasticity. In this review, we delve into the origins of ECM and cell viscoelasticity, examine recently developed methods for measuring ECM and cell viscoelasticity, and summarize the potential interactions between cell and ECM viscoelasticity. Recent research has shown that both ECM and cell viscoelasticity experience alterations during *in vivo* pathogenesis, indicating the potential use of tailored viscoelastic ECM and cells in regenerative medicine.

## 1. Introduction

Tissues comprise cells, extracellular matrix, and extracellular fluid. While previous research has emphasized the study of tissues' elastic properties,<sup>1,2</sup> recent advances in understanding the *in vivo* environment have revealed the widespread presence of viscoelasticity in most tissues, including soft tissues (e.g., liver, breast, muscle, skin, and adipose tissue)<sup>3–8</sup> and hard skeletal tissues (e.g., bones, tendons, ligaments, and cartilage).<sup>9–12</sup> Viscoelasticity in tissues is attributed to both the extracellular matrix and cells. The viscoelasticity of the ECM primarily arises from stress relaxation and creep behavior due to weak bonds between the fibrin polymeric network and attached macromolecules.<sup>13,14</sup> Conversely, the viscoelasticity of cells primarily results from high water content and the cytoskeleton within cells.<sup>15</sup> For instance, the brain can dissipate nearly as much energy as its storage modulus.<sup>16</sup> Evidence suggests that viscoelasticity plays a crucial role in biogenesis processes. Studies have indicated that mesenchymal stem cells (MSCs) cultured on hydrogels with different viscoelastic properties exhibit distinct differentiation trends and cellular activities.<sup>17</sup> Furthermore, the spreading and proliferation of C2C12 cells can be modulated by viscoelastic hydrogels.<sup>18</sup>

In recent years, there has been a proliferation of experimental

techniques designed to investigate the viscoelastic properties of materials and cells. Examples include magnetic tweezers and magnetic twist cytometry,<sup>19–23</sup> which have emerged as qualitative methods for assessing the viscoelasticity of both extracellular matrix (ECM) and cells, following pioneering work by Crick and Hughes in 1950. Similarly, the micropipette aspiration method,<sup>24,25</sup> introduced by Mitchison and Swann in 1954, can be used to qualitatively measure the viscoelasticity of cells and artificial microspheres. Additionally, technologies such as atomic force microscopy (AFM),<sup>26</sup> cytoindenter,<sup>27</sup> and optical tweezers<sup>28,29</sup> or laser traps are gradually being adopted by different laboratories to explore the viscoelastic properties of various materials. However, inconsistencies in measurement modes, experimental parameters, and other factors make it challenging to compare results from different studies, leaving substantial room for interpretation. Therefore, there is a pressing need to summarize the various test methods for ECM and cell viscoelasticity, understand the differences and relationships among experimental parameters, and establish common standards to harmonize the scope of these diverse studies.

The primary emphasis in early research on how extracellular matrix (ECM) mechanical properties affect cells has been on the elasticity of ECM.<sup>30–32</sup> However, recent research has highlighted the role of

\* Corresponding author.

E-mail address: [duyanan@tsinghua.edu.cn](mailto:duyanan@tsinghua.edu.cn) (Y. Du).<https://doi.org/10.1016/j.mbm.2024.100082>

Received 9 March 2024; Received in revised form 14 July 2024; Accepted 15 July 2024

Available online 31 July 2024

2949-9070/© 2024 The Authors. Published by Elsevier B.V. on behalf of Shanghai Ninth People's Hospital, Shanghai Jiao Tong University School of Medicine. This is an open access article under the CC BY-NC-ND license (<http://creativecommons.org/licenses/by-nc-nd/4.0/>).

viscoelasticity in various physiological processes, such as cell spreading, proliferation, differentiation, and metabolism.<sup>33–35</sup> This is achieved by regulating the viscoelastic properties of hydrogels with adjustable stress relaxation. Cell mechanics, specifically the forces that cells exert and experience, have profound impacts on the extracellular matrix (ECM). The cell's mechanical properties, such as stiffness, can modulate the ECM's structure and composition, influencing tissue development, homeostasis, and disease.<sup>36,37</sup> In this review, we provide an overview of the origin of viscoelasticity in both the ECM and cells, discuss methods for measuring their viscoelasticity, and explore potential interactions between these two key components of native tissues. Additionally, we address the challenges in this field. The development of engineered cells and microenvironments with customizable viscoelasticity holds promise for advancing in vitro studies on cell-ECM interactions and for furthering the fields of tissue engineering and regenerative medicine with potential clinical applications.

## 2. Origin of ECM and cell viscoelasticity

### 2.1. Origin of ECM viscoelasticity

Viscoelasticity is a prevalent characteristic of living tissue and the extracellular matrix (ECM), characterized by immediate elasticity in response to external mechanical disturbances, followed by time-dependent mechanical response and energy dissipation. Viscoelastic materials deform over time when subjected to external loads and undergo stress relaxation in response to those loads. Energy dissipation in tissue and the ECM is influenced by various factors, with the ECM, comprising a polymeric network of collagen, fibrin, and highly hydrated, flexible polysaccharides and other macromolecules (Fig. 1), being the primary contributor to tissue viscoelasticity.<sup>38</sup> Dissipation in the collagen or fibrin network is affected by the properties of the bonds linking the fibers.<sup>13,14</sup> The presence of a non-covalently crosslinked network and weak bonds with fast dissociation rates can result in time-dependent

viscoelastic behavior, such as creep and stress relaxation. These weak bonds also exhibit nonlinear mechanical behavior, consuming energy under external mechanical deformation and loading. The reformation of weak bonds within the ECM following deformation can stabilize it in a deformed state, resulting in plastic deformation. Recent studies have indicated that the viscoelasticity of the collagen network is due to the formation of new crosslinks. However, applying large strains for short periods of time or moderate strains at low rates can lead to permanent fiber elongation.<sup>39</sup> The dissipation mechanism has been observed in tissues under mechanical loading, such as skin and tendon tissues, where bond sliding between collagen fibers and sliding of collagen fibrils have been observed in vivo, resulting in viscoelastic behavior.<sup>40,41</sup> Another mechanism is the entanglement of polymers, which allows the release of energy and enables the matrix to flow. In tissue or the extracellular matrix (ECM), weak bonds or entanglements coexist with more stable covalent crosslinks, reducing the liquid-like flow and mechanical plasticity throughout the matrix.<sup>42</sup> The unfolding of proteins is also a mechanism for energy dissipation as seen in vitro in fibrin, spectrin, and intermediate filament networks.<sup>43,44</sup> To mimic the viscoelastic properties of natural tissues in bioengineered materials, researchers have developed energy-dissipating hydrogels. These hydrogels are typically composed of protease-resistant polymers that do not adhere to cells. To achieve the desired viscoelasticity, cell adhesion peptide motifs or proteins can be attached to the polymers.<sup>45–47</sup> In contrast, pure elastic hydrogels form ideal polymer networks, while incompletely crosslinked polymeric networks in non-ideal cross-linked hydrogels lead to energy dissipation and creeping.<sup>48</sup> Varying concentrations of acrylamide (monomer) and bis-acrylamide (crosslinking agent), or the addition of a non-crosslinked linear acrylamide polymer to a crosslinked polyacrylamide gel, can be employed to produce gels with consistent storage modulus but different loss moduli.<sup>49,50</sup> Furthermore, viscoelasticity can be tailored by integrating weak bonds into the polymer network. For example, viscoelastic PEG hydrogels can be synthesized using dynamic covalent hydrazone bonds, boronate bonds, or thioester exchange.<sup>3,51–53</sup> In alginate gels,

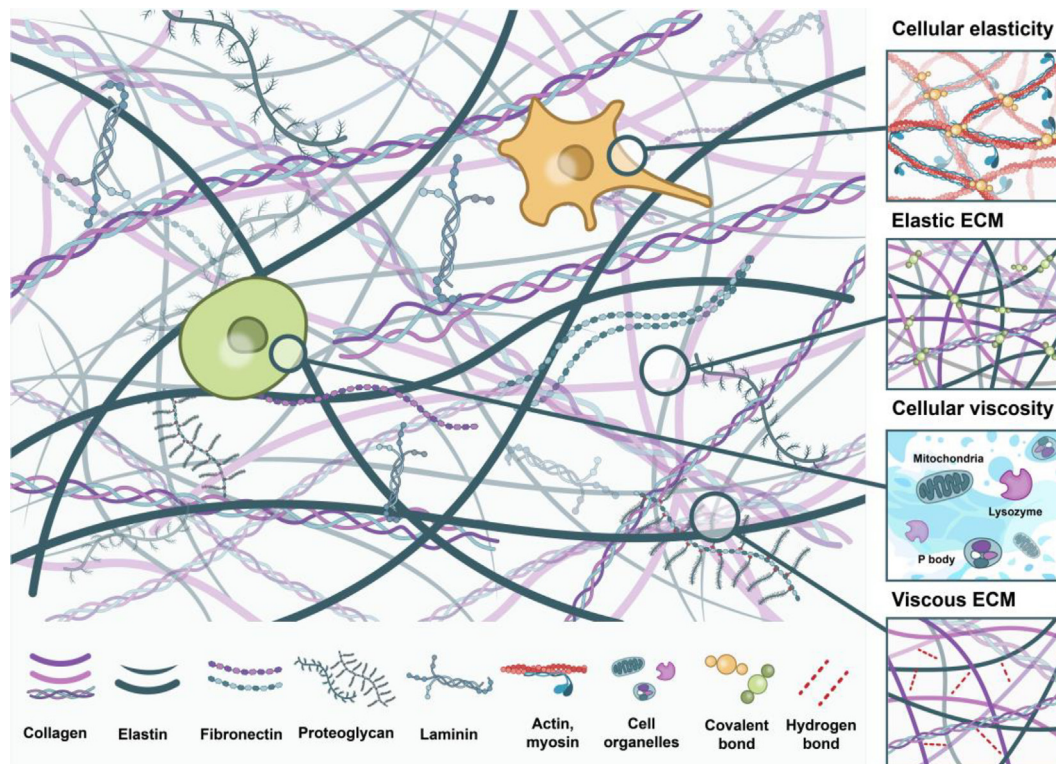


**Fig. 1.** The viscoelasticity of ECM and cell. ECM elasticity is mainly derived from covalent interactions between collagen and elastin networks while the viscous part comes from the weak interaction force and bond slippage. Cell viscoelasticity mainly depends on the cytoskeleton and the high-water content.

weak ionic crosslinking induces viscoelastic behavior.<sup>17,54</sup> Viscoelastic hyaluronic acid-based hydrogels can be formed through hydrazone bonds or guest-host crosslinking.<sup>35,55</sup> Peptide-based hydrogels can integrate weak crosslinks, enabling independent adjustment of viscoelasticity and initial elastic modulus by modifying parameters such as constituent polymer molecular weight, inert molecule coupling as spacers, bond strength, weak-to-covalent bond ratio, and total bond count.<sup>17,34,35,55–58</sup>

## 2.2. Origin of cell viscoelasticity

Living cells demonstrate viscoelastic behavior, functioning as both elastic solids and viscous fluids due to their high water content and polymeric structural matrix. The viscoelastic properties of cells are influenced by their cellular components, including the cell membrane, cytoskeleton, and cytoplasmic viscosity (Fig. 1). The cytoskeleton, comprising microtubules, intermediate filaments, and microfilaments, significantly determines cell viscoelasticity.<sup>15</sup> Empirical evidence has established the cytoskeleton as a major factor in cell viscoelasticity.<sup>59–61</sup> Cytoskeletal viscoelasticity involves two main mechanisms. Firstly, local cytoskeletal contraction can induce intracellular poroelastic effects and transient pressure gradients over biologically relevant timescales.<sup>62–64</sup> Secondly, the cytoskeletal filaments are held together by few or non-covalent bonds. Kinesins apply random athermal forces on the cytoskeletal filopodia, leading to faster movement compared to thermal agitation.<sup>65</sup> This results in activated cytoskeletons being more fluid than those without kinesin.<sup>66</sup> The cytoskeleton, serving as the fundamental biopolymer scaffold of living cells, maintains a balance between dynamic reorganization and cell body maintenance through its viscoelastic properties. Changes in cell-scale viscoelasticity play a crucial role in cellular physiology, impacting cell morphology, motility, and division.<sup>59,60</sup> Moreover, cellular viscoelasticity influences tissue scale phenomena, such as postmortem muscle stiffening and coagulation, which is partly attributed to increased connections between actin filaments and myosin. Living muscle hydrolyzes ATP to facilitate rapid formation and dissociation of actin–myosin junctions.<sup>67</sup>

## 3. Measurement of ECM and cell viscoelasticity

In recent years, numerous experimental methods have been employed to measure the viscoelasticity of ECM and cells. However, due to inherent differences among these methods, there is considerable variation in the experimental results they yield. Here, we provide a summary of the experimental techniques used for measuring the viscoelastic properties of ECM and cells (Table 1).

### 3.1. Measurement of ECM viscoelasticity

The methods for measuring ECM viscoelasticity are primarily divided into bulk and local viscoelasticity measurements. Bulk viscoelasticity measurement methods include rheometer, stretcher, compressor, NMR, and ultrasound. Local viscoelasticity measurement methods include AFM, nano indenter, optical tweezer, and magnetic tweezer (Fig. 2).

#### 3.1.1. Dynamic rheometer

Dynamic rheometry was initially used to analyze the rheological characteristics of materials in order to measure their response to external forces. In conventional rheometer testing, there are primarily two methods for assessing the viscoelastic properties of materials. These methods include static mechanical testing, such as stress relaxation and creep tests, and dynamic mechanical testing, such as frequency-dependent rheology tests.<sup>68</sup> During static mechanical testing, stress relaxation experiments were conducted with the goal of maintaining a specific strain ( $\epsilon_0$ ) in order to observe how the internal stress of the elastic material decreases over time,  $\sigma(t)$ . The creep test subjected the

elastic material to constant stress ( $\sigma_0$ ) for an extended period, observing the gradual increase in strain over time,  $\epsilon(t)$ . When undergoing dynamic mechanical testing, a viscoelastic material retains some of the energy as shear stress, termed as the storage modulus ( $G'$ ), allowing the material to preserve its initial shape. The remaining energy is dissipated through the material's viscous components, known as the loss modulus ( $G''$ ). The composite shear modulus can be calculated using the formula:<sup>69</sup>  $|G^*| = \sqrt{G'^2 + G''^2}$ . Additionally, the damping ratio ( $\zeta$ ) can be determined as the ratio of  $G''$  to  $G'$ . Recent studies have employed dynamic rheometry methods to assess the viscoelastic characteristics of tissues and biomaterials. Studies have indicated that soft tissues typically exhibit loss moduli ranging from 10% to 20% of their storage modulus at 1 Hz.<sup>42</sup> Rheological testing has shown that the shear modulus of connective tissue is approximately 690 Pa, while the shear modulus of fatty tissue is only 290 Pa.<sup>70</sup> Rheometers are also commonly used to determine the stress relaxation time of various tissues and hydrogels. Stress relaxation tests have demonstrated that the stress relaxation times of soft tissues such as liver, breast, muscle, skin, and adipose tissue range from tens to hundreds of seconds.<sup>42</sup> Mooney's group has utilized rheometry techniques to measure the stress relaxation times of sodium alginate hydrogels, which range from 100 to 1000s.<sup>17</sup>

#### 3.1.2. Stretcher

Tensile tests are conducted using an extensometer to evaluate the viscoelastic properties of biomaterials, and these tests are carried out on a standard traction-compression machine in displacement mode. Deformation measurements are taken using an extensometer during the tests.<sup>71</sup> A stress–strain curve is obtained for each test specimen after being subjected to loading in the uniaxial tensile test. To analyze the viscoelastic behavior of the material, a three-layer structure is used based on the Kelvin-Voigt model, using a spring and punch configuration.<sup>72</sup> The stress relaxation modulus  $E(t)$  can be determined using the equation

$$E(t) = \frac{\sigma(t)}{\epsilon_0}$$

The behavior of the aortic valve is influenced by the time-dependent stress,  $\sigma(t)$ , and the applied strain,  $\epsilon_0$ . When experimental data is extrapolated to the physiological strain rate, previous studies have revealed that the viscous damping coefficients of the aortic valve are 8.3 MPa and 3.9 MPa in the circumferential and radial directions, respectively.<sup>73</sup> Furthermore, it has been demonstrated that the stress relaxation modulus in normal bone is approximately 9 MPa, but decreases to around 7 MPa in the presence of osteoporosis.<sup>73</sup>

#### 3.1.3. Compressor

Probe indentation is a commonly employed technique for deforming soft tissues and biological materials, enabling the evaluation of their response to applied stresses.<sup>74</sup> This is typically done through compression creep tests and compression stress relaxation tests, which yield the creep compliance function  $J(t)$  and stress relaxation modulus  $E(t)$  used to characterize the viscoelastic behavior of the materials. The compliance function  $J(t)$  can be determined by calculation.

$$J(t) = \frac{\epsilon(t)}{\sigma_0}$$

The time-dependent strain  $\epsilon(t)$  and applied stress  $\sigma_0$  are represented by the variables in this context. Experimental data extrapolation to the physiological strain rate has revealed viscous damping coefficients of 8.3 MPa and 3.9 MPa in the circumferential and radial directions, respectively, for the aortic valve.<sup>75</sup> The indentation stress relaxation modulus during compression tests can vary from a few kPa to several hundred kPa. In aortic valve testing, a stress of 125 kPa is applied in these experiments.<sup>74</sup>

**Table 1**  
Comparison of Different tools for measuring viscoelasticity.

Measurement	Dimension	Technology	Concept	Modulus	Parameter relationship	Example	Refs
Measurement for ECM viscoelasticity	Bulk	Stretcher	Classic stress-strain analysis. Uniaxial stress is applied to stretch the material and a relationship is established with the resulting strain	E (elastic)	$E(t) = \frac{\sigma(t)}{\varepsilon_0}$	E: 8.3 MPa (aortic valve); 1.23 MPa (spinal cord)	71–73
		Compressor	Classic stress-strain analysis. Uniaxial stress is applied to compress the material and a relationship is established with the resulting strain	E (elastic)	$J(t) = \frac{\varepsilon(t)}{\sigma_0}$	E: 125 kPa (aortic valve); 0.5–1.5 kPa (spinal cord)	74,75
		Rheometer	Application of small-amplitude oscillatory shear stress and quantification of the resulting strain	E (elastic) G', G'' (viscoelastic) $\tau$ (stress relaxation)	$G^* = \sqrt{G'^2 + G''^2}$	G': 0.83 kPa (Brain); 1.3 MPa (Cartilage)	12,17,68,70
		NMR	Magnetic resonance visualization of tissue deformation resulting from the introduction of shear waves into the tissue derived from external vibrations	G', G'' (viscoelastic)	$E = T/S$	G': 9.8 kPa (lung)	76–78
		Ultrasound	Ultrasonic pulses produce shear waves through the tissue; the velocity of these waves is measured and used to derive the tissue's Young's modulus	E (elastic) G', G'' (viscoelastic)	$E = T/S$	E: 1 MPa ( skin )	2,79
	Local	AFM	uses a sharp probe to measure the forces between the probe tip and the sample surface, providing information about the surface's mechanical properties at the atomic scale		$E(t) = E_0 t^\beta$	E: 322 kPa (skin)	80–84
		Nano indenter	Indentation of the tissue with a probe of defined geometry and calculation of the relationship between indentation depth and probe load (the probe must be smaller than the sample)	E (elastic) $\beta$ (viscoelastic) $\tau$ (stress relaxation)	$h(t)^2 = \frac{\pi}{2} P_0 \cot \alpha \left[ \frac{1}{E_1} + \frac{1}{E_2} (1 - e^{-tE_2/\eta_1}) + \frac{1}{\eta_2} t \right]$	E: 17.8 GPa (trabecular bone); 20 GPa (cortical bone)	27,30,85
		Optical tweezer	light enters a medium of a different refractive index the light path changes	E (elastic) G', G'' (viscoelastic) $\tau$ (stress relaxation)	$G'(\omega) = \frac{k_{OT}}{6\pi a} \left( \frac{A \cos \delta(\omega)}{D(\omega)} - 1 \right)$ $G''(\omega) = \frac{k_{OT}}{6\pi a}$	G': 5–1000Pa (melanoma tumors)	86–89

(continued on next page)

Table 1 (continued)

Measurement	Dimension	Technology	Concept	Modulus	Parameter relationship	Example	Refs
Measurement for Cell viscoelasticity	Single Cell/Subcellular	Magnetic tweezer	the magnetophoretic motion of the beads subjected to a constant magnetic force	E (elastic) μ (shear viscoelastic)	$\left(\frac{A \sin \delta(\omega)}{D(\omega)}\right)$ $\mu = \frac{E}{2(1 + \sigma)}$	E:0.5–30 kPa (Fibroblast)	22,90
		AFM		E (elastic) β(viscoelastic) τ (stress relaxation)	$E = T/S$	E:0.5 kPa (alveolar cells) 0.7 kPa (bronchial cells)	83,91–93
		Nano indenter		E (elastic) β(viscoelastic) τ (stress relaxation)	$F = \frac{3EI}{L^3} \delta$	E: 2.5 kPa (MSC)	94
		QDC	analyze and quantify the mechanical properties of cells, such as cell stiffness and deformability, by subjecting them to controlled flow conditions within microchannels.	E (elastic) β ( viscoelastic )	$E = T/S$	β: 0.6 (macrophage)	100–102
		micropipette aspiration		E (elastic) β ( viscoelastic )	$E = T/S$	E: 0.89 kPa (osteogenic MSC), 0.22 kPa (adipogenic MSC)	103–105
		Optical tweezer/Optical stretcher		E (elastic) G', G'' (viscoelastic) τ (stress relaxation)	$G'(\omega) = \frac{k_{OT}}{4\pi a} \left( \frac{3}{2 \sin \theta} + \frac{\cos \theta}{\sin^3 \theta} \right)$ $\left( \frac{A \cos \delta(\omega)}{D(\omega)} \right) - 1$ $G''(\omega) = \frac{3k_{OT}}{16 a \sin \theta} \left( \frac{A \sin \delta(\omega)}{D(\omega)} \right)$	Neurons: 50 Pa ≤ G' ≤ 136Pa, 23Pa ≤ G'' ≤ 84Pa Astrocytes: 32Pa ≤ G' ≤ 100Pa, 19Pa ≤ G'' ≤ 59Pa	28,95,96
		Magnetic tweezer	Obtain mechanical properties through microbeads via which a magnetic torque is applied	E (elastic) μ (viscoelastic)	$G^* = \sqrt{G'^2 + G''^2}$	μ: 210 Pa s (macrophage)	20,22,97
		Magnetic twisting cytometry		E (elastic) G', G'' (viscoelastic) τ (stress relaxation)	$G^* = \sqrt{G'^2 + G''^2}$	G':0.55 kPa (naive ESC), ≤2 kPa (differentiated ESC)	23,98,99
		Brillouin Microscopy		Brillouin shift			106



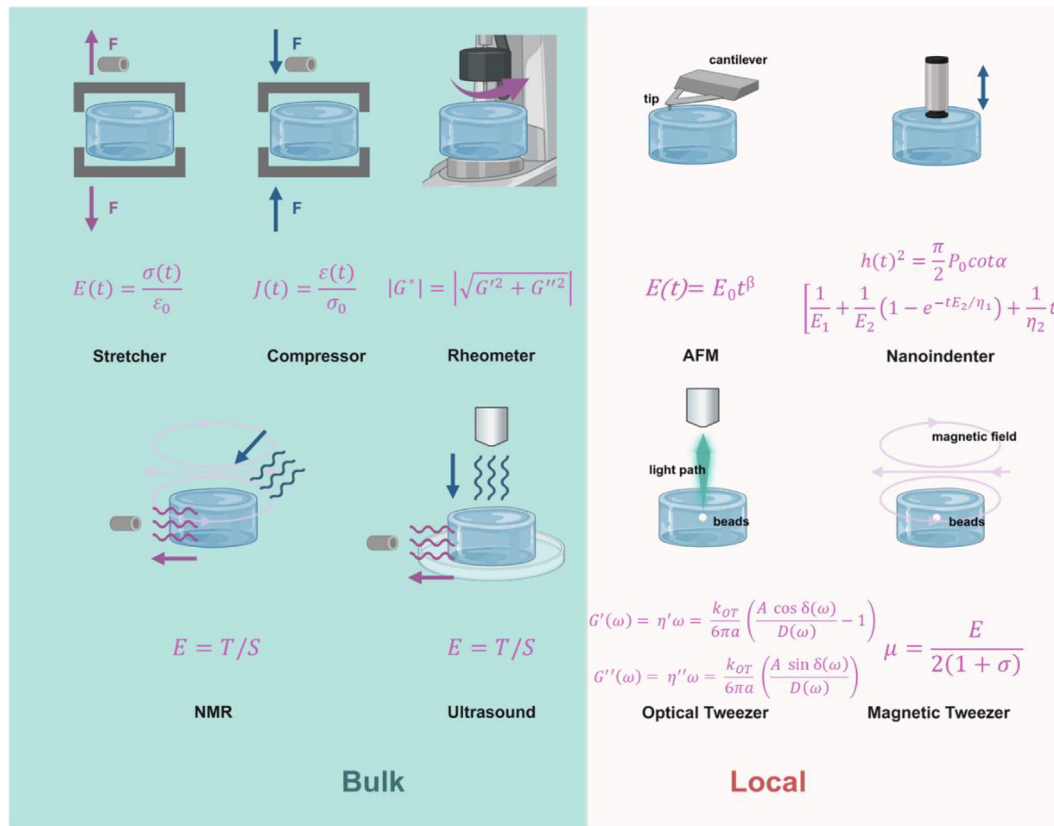


**Fig. 2.** Measurement tools for ECM viscoelasticity. Schematic diagram and formula for bulk measurement (e.g. stretcher, compressor, rheometer, NMR, ultrasound) and local measurement (e.g. AFM, nano indenter, optical tweezer, magnetic tweezer) tools for ECM viscoelasticity.

### 3.1.4. NMR

Nuclear magnetic resonance (NMR) methods are used for monitoring and mapping the elastic properties of tissues.<sup>76</sup> It was shown that the relationship between the second moment of the 1H NMR absorption line and the slope of the strain and strain–stress relationship curves at high strain values in vascular tissues. It is proposed that NMR relaxation times can be used to detect the stress state of tissues. Recent studies have revealed systematic characterization of the underlying microstructural changes on different organs and processes such as liver fibrosis, neuronal tissue degeneration and muscle contraction by using ultrasound and magnetic resource imaging (MRI).<sup>77</sup> Studies have demonstrated that tissue degeneration in the brain is associated with a decrease in the viscoelastic parameters  $\mu$  and  $\alpha$ . Additionally, chronic muscle has been shown to have a significant effect on tissue viscoelasticity, with a decrease of 20.46% in  $\mu$  and 6.07% in  $\alpha$ .<sup>78</sup> Other researchers have utilized 3D MR elastography to measure the shear modulus of tissues, finding that the pancreas has a shear modulus of approximately 1.15 kPa, while the liver has a higher value of around 1.6 kPa.<sup>76</sup>

### 3.1.5. Ultrasound

The elastic properties of soft tissues are influenced by their molecular constituents and organization at the micro- and macro-structural scale (cite). Common ultrasound imaging techniques rely on differences in acoustic impedance among body tissues. However, the impedance echo signal poses challenges in distinguishing tissues with the same acoustic impedance. For instance, breast tumors and healthy cystic tissues appear faint in B-MODE and are difficult to differentiate.<sup>78</sup> Ultrasound elastography is an innovative application of ultrasound technology, initially proposed by Ophir et al. in 1991. It primarily examines the correlation between tissue's elastic modulus and its biological properties for imaging purposes (cite). The elastic modulus of a tissue can be expressed by the formula  $E = T/S$ , where  $E$  represents the elastic modulus,  $T$  represents the

stress, and  $S$  represents the strain. Ultrasound elastography applies either external or internal static/dynamic pressure to the tissue, including inner body movements like breathing and heartbeat. By utilizing ultrasound imaging methods in conjunction with digital signal processing and digital image processing techniques, it is possible to estimate the corresponding changes in internal displacement, strain, velocity, and other tissue parameters, thus obtaining the distribution of mechanical properties such as the elastic modulus.<sup>79</sup> A study has demonstrated that the average Young's modulus, as measured by ultrasonic shear wave elastography, is 14.8 GPa and 20.7 GPa for individual trabeculae and cortical bone, respectively.<sup>2</sup>

### 3.1.6. AFM

Atomic Force Microscopy (AFM) was invented in 1986 and has since become a widely used tool for measuring the mechanical properties of materials and cells. AFM's ability to accurately apply forces and disturbances at the picoscale has made it particularly valuable for these types of measurements.<sup>80</sup> In a traditional AFM system, a soft mechanical cantilever and a sharp probe are attached to the device, which is then used to touch the surface of the sample. When performing pressure experiments, AFM uses the mechanical cantilever to measure force displacement by applying a small pressure in a direction perpendicular to the sample surface. Young's modulus can be determined using analytical theories, such as the Hertzian contact model, based on the indentation loading curve.<sup>81</sup> While force-displacement curves are commonly used in AFM to measure the local, nanoscale elastic properties of soft materials, a theoretical framework for extracting viscoelastic constitutive parameters from force-displacement data has been lacking.<sup>82</sup> Recent advancements have validated an approach based on the principle of elastic-viscoelastic correspondence through finite element (FE) simulations and comparison with existing in vivo cell and hydrogel AFM techniques. Using this approach, viscoelastic model parameters such as the relaxation time ( $\tau$ )

for the standard linear solid (SLS) model or the power-law decay exponent ( $\alpha$ ) for the power-law rheology (PLR) model can be calculated by fitting the data.<sup>83</sup> For example, AFM was used to obtain nanoscale viscoelastic data for PAAM hydrogels using the SLS model with a relaxation time ( $\tau$ ) of 0.01 s and the PLR model with an alpha ( $\alpha$ ) value of 0.12.<sup>80</sup> In terms of tissue, AFM has been used to measure the Young's modulus of normal skin, which was found to peak at approximately 322 kPa and range from 25.8 kPa to 1.18 MPa. The relaxation time for the SLS model was determined to be 3 s.<sup>84</sup>

### 3.1.7. Nano indenter

Nanoindentation is a valuable technique for characterizing the mechanical properties of biomaterials and tissues at a submicron level.<sup>27</sup> The Burger model is commonly used in creep tests to determine the viscoelastic properties of these materials.<sup>85</sup> According to this model, the penetration depth ( $h$ ) increases with time according to the following equation:

$$h(t)^2 = \frac{\pi}{2} P_0 \cot \alpha \left[ \frac{1}{E_1} + \frac{1}{E_2} (1 - e^{-t/\eta_2}) + \frac{1}{\eta_2} t \right]$$

In this equation,  $P_0$  represents the peak force,  $\alpha$  is the equivalent cone half-angle,  $E_1$  and  $E_2$  are the moduli measured in gigapascals (GPa),  $\eta_2$  is the long-term creep viscosity measured in GPa, and  $1/E_2$  is the creep time constant measured in seconds (s).<sup>30</sup> Recent research has indicated that the creep time for both cortical and trabecular bone at the sub-microscopic level is approximately 60 s.<sup>85</sup> Furthermore, the storage modulus for trabecular bone was found to be 17.8 GPa, while the storage modulus for cortical bone was found to be 20.0 GPa.<sup>27</sup>

### 3.1.8. Optical tweezers

In recent years, optical tweezers have been widely used for measuring the mechanical properties of biological materials, cells, and biomolecules.<sup>86</sup> Typically, microspheres of varying sizes are utilized as light traps to capture objects. The study of mechanical properties involves measuring both the specific and non-specific binding of the object. In general, position-sensitive detectors based on four-quadrant photodiodes are employed by optical tweezers for accurately detecting the position of microspheres in terms of spatial and temporal accuracy.<sup>86</sup> For mechanical calibration, microspheres that are not bound to the object being tested and are free in solution are used. The optical trap stiffness, denoted as  $k$ , is determined by examining the time-dependent thermodynamic perturbations of the microspheres.<sup>87</sup> Using optical tweezers, the viscoelastic energy of the biological material can be calculated by directly measuring the displacement ( $D$ ) and phase shift ( $\delta$ ) of particle motion in response to the oscillation trap. The expression for calculating the viscoelastic energy is given by:<sup>88</sup>

$$G'(\omega) = \eta' \omega = \frac{k_{OT}}{6\pi a} \left( \frac{A \cos \delta(\omega)}{D(\omega)} - 1 \right)$$

$$G''(\omega) = \eta'' \omega = \frac{k_{OT}}{6\pi a} \left( \frac{A \sin \delta(\omega)}{D(\omega)} \right)$$

A recent study has found that both mouse melanoma tumors and human breast tumors exhibit complex moduli ranging from 5 to 1000 Pa. Specifically, the storage modulus of a PEG-LMWH hydrogel was approximately 30 Pa, while the loss modulus was around 2 Pa.<sup>89</sup>

### 3.1.9. Magnetic tweezers

Magnetic tweezers commonly utilize a magnetic sphere as the target of magnetic force. Through appropriate modification of the magnetic ball, it can be specifically combined with the test sample, and subsequently a magnetic field is applied to the ball for the purpose of analyzing the mechanical properties of the test sample.<sup>22</sup> Generally, magnetic tweezers determine the velocity at which a magnetic bead approaches a pole piece in a liquid with known viscosity under different coil currents.

This allows for the calibration of the correlation between the force exerted on the magnetic sphere and the distance it travels using Stokes' law. In the context of magnetic tweezer experiments, the viscosity coefficients are typically acquired through creep response experiments. By employing these experiments, the shear modulus can be calculated using the equation

$$\mu = \frac{E}{2(1 + \sigma)}$$

To illustrate the effectiveness of magnetic tweezers, a recent study reported a shear modulus of 0.03 Pa for F-actin solutions.<sup>90</sup>

## 3.2. Measurement of cell viscoelasticity

There are various methods for measuring cell viscoelasticity, including traditional techniques like AFM, nano indenter, magnetic twisting cytometry, magnetic tweezer, optical tweezer, micropipette aspiration, as well as newer developments such as QDC and Brillouin microscopy (Fig. 3).

### 3.2.1. AFM

Atomic Force Microscopy (AFM) is a highly precise technique used for surface characterization. It has gained popularity in the field of biology for its ability to image and analyze various biological samples with great detail. One area where AFM is extensively employed is in studying the mechanics of cells. AFM force spectroscopy, for instance, is utilized for measuring cellular elasticity and rheology.<sup>91</sup> In addition, stress relaxation, creep experiments, and oscillation tests can be readily conducted to gather information on the mechanical properties of cells over time.<sup>83</sup> Recent examinations of AFM indentation and stress relaxation assays have shown that cells respond to mechanical stimulation in a manner consistent with the theory of "poroelasticity," similar to the behavior exhibited by organs in the body.<sup>92</sup> To illustrate, the AFM rheology system was employed to measure the shear modulus of lung cells, resulting in a measurement of 0.5 kPa for alveolar cells and 0.7 kPa for bronchial cells.<sup>93</sup>

### 3.2.2. Nano indenter

The nanoindentation technique has been developed as a dynamic indentation test to enhance the capabilities of existing indentation methods. This method utilizes both sinusoidal loading and quasi-static loading to conduct a wide range of tests. In brief, according to the theory for a cylindrical cantilever beam, the bending of the beam can be related to the reaction force by the equation:

$$F = \frac{3EI}{L^3} \delta$$

where  $E$  (Young's modulus),  $I$  (moment of inertia), and  $L$  (length of the cantilever beam) are known.<sup>93</sup> A study demonstrated that by using a cell-indentation apparatus (cytoindenter), the shear modulus of MG63 osteoblast-like cells was found to be 2 kPa. This value is two to three orders of magnitude smaller than that of articular cartilage, six to seven orders smaller than that of compact bone, and quite similar to that of leukocytes.<sup>94</sup>

### 3.2.3. Optical tweezers

The use of optical methods for cell imaging has a long history. In recent years, there has been a growing interest in cell mechanics, leading to the development of several methods that utilize light trapping to manipulate cells.<sup>28</sup> The conservation of momentum ensures that light passing through a material experiences a restoring force, allowing for the trapping and manipulation of cells or beads using collimated light sources.<sup>95</sup> Traditionally, two models have been used to measure cell viscoelasticity. In intracellular measurements, an internal granule is trapped and oscillated to determine  $G'$  and  $G''$ . These values are obtained

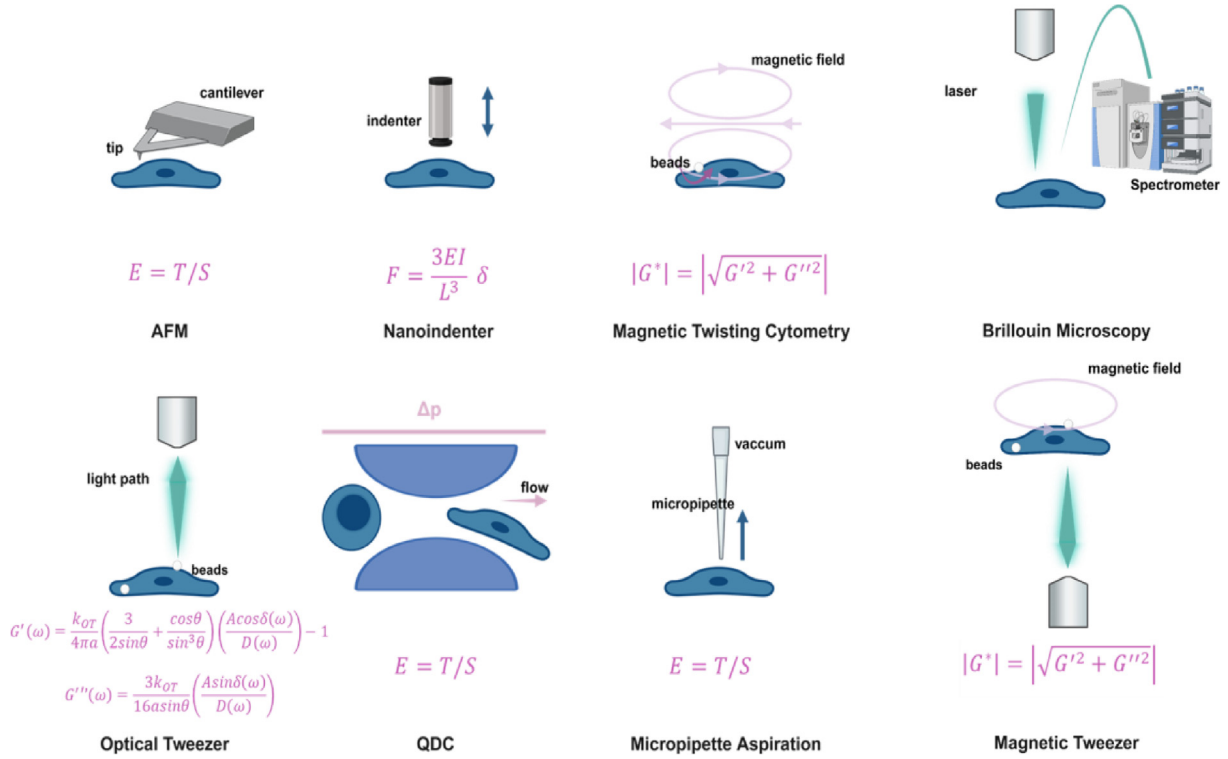


**Fig. 3.** Measurement tools for cell viscoelasticity. Schematic diagram and formula for measuring cell viscoelasticity (e.g., AFM, nanoindenter, magnetic twisting cytometry, optical tweezer, QDC, micropipette aspiration).

from experimentally measured particle displacement magnitude ( $D$ ) and phase shift ( $\delta$ ) using the equations provided

$$G'(\omega) = \frac{k_{OT}}{6\pi a} = \frac{k_{OT}}{6\pi a} \left( \frac{A\cos\delta(\omega)}{D(\omega)} \right) - 1 \quad G''(\omega) = \frac{k_{OT}}{6\pi a} \left( \frac{A\sin\delta(\omega)}{D(\omega)} \right)$$

In extracellular measurements, uncoated beads attached to the cell surface are trapped and oscillated. The storage modulus  $G'$  and the loss modulus  $G''$  of the cell are determined using the equations provided

$$G'(\omega) = \frac{k_{OT}}{4\pi a} \left( \frac{3}{2\sin\theta} + \frac{\cos\theta}{\sin^3\theta} \right) \left( \frac{A\cos\delta(\omega)}{D(\omega)} \right) - 1$$

$$G''(\omega) = \frac{3k_{OT}}{16a\sin\theta} \left( \frac{A\sin\delta(\omega)}{D(\omega)} \right)$$

Studies have shown that neurons have an elastic modulus ranging from 50 to 136 Pa and a viscous modulus ranging from 23 to 84 Pa. Astrocytes, on the other hand, have an elastic modulus ranging from 32 to 100 Pa and a viscous modulus ranging from 19 to 59 Pa. This suggests that the soft nature of astrocytes may be better suited to provide support for neurons, as neurons prefer softer substrates for proliferation and differentiation. It is worth noting that neurons can also change their mechanical properties during growth and development.<sup>96</sup>

### 3.2.4. Magnetic tweezers

Magnetic beads, microspheres, and rods offer the opportunity to introduce precise and localized forces into specific cellular compartments. Magnetite, magnetite/nickel, and cobalt alloy nanoparticles (NPs), microspheres, and rods enable the application of these forces to specific cellular compartments as well as surface receptors like integrins and catenin structures.<sup>97</sup> These materials have facilitated the quantification of mechanical properties of the cytoplasm and nucleus, and have been employed to study mechanotransduction pathways. Consequently, magnetic beads (MBs) possess unique qualities that distinguish them from other micro- and NPs. When these beads are subjected to an external

magnetic field (MF), they generate forces within the physiological range observed in vivo (10–12 to 10–9 N).<sup>20</sup> Additionally, they can be easily synthesized in various sizes, ranging from nanoscale spherical particles to micron-sized beads and rods, with excellent control over their shape, crystallinity, and size uniformity. MBs can be produced as either single superparamagnetic NPs or multi-domain ferromagnetic beads, which can be functionalized with specific ligands to target specific receptors. Magnetic tweezers employ a magnetic field gradient to pull individual beads, allowing for high spatial resolution manipulation of 1 MB at a time and the ability to track its motion during magnetic stimulation. By utilizing magnetic tweezers, the shear modulus of macrophages can be measured. The shear modulus values exhibit significant variability within the cell population, ranging from 20 to 735 Pa (averaging at 343 Pa), and a factor of 2 variation within individual cells. The cytoplasm's effective viscosity displays a relatively sharp distribution, with an average value of  $\eta = 210 \text{ Pa s}$  ( $\pm 143 \text{ Pa s}$ ).<sup>22</sup>

### 3.2.5. Magnetic twisting cytometry

Magnetic torsion cytometry (MTC) is a valuable technique for investigating cellular micromechanics. In MTC, modified magnetic beads (typically RGD-coated ferromagnetic microbeads) are used. These beads bind specifically to the integrin transmembrane receptor, which is known to be associated with the actin cytoskeleton.<sup>23</sup> In conventional magnetic torsion cytometry experiments, microbeads linked to integrins and, consequently, to the cytoskeleton, are used to apply a magnetic moment directly to the cell surface. The magnetic field is oriented horizontally, parallel to the cell monolayer. This orientation allows for the generation of a perpendicular magnetic moment by a Helmholtz coil, which produces a uniform field strength that facilitates the rotation of the magnetic sphere. This rotation provides the corresponding viscoelastic parameters. Recent research has applied MTC in combination with optical tweezers to evaluate the viscoelastic properties of adherent alveolar epithelial cells. It was found that the  $E$  values obtained using MTC ( $\sim 34$ – $58 \text{ Pa}$ ) were smaller than those obtained using optical tweezers ( $\sim 29$ – $258 \text{ Pa}$ ). However, the relaxation time constants were similar for both techniques,



approximately 2 s.<sup>98</sup> Another study revealed that the shear modulus of naive embryonic stem cells is 0.55 kPa, while that of differentiated embryonic stem cells is approximately 2 kPa.<sup>99</sup>

### 3.2.6. QDC

The QDC microfluidic device comprises of a bifurcated channel network that extends into a parallel array of 16 channels containing micrometer-scale constraints. In the QDC experiment, cells are initially impeded by spatial constraints as they traverse the first narrow channel in the microfluidic characterization zone. However, under fluid pressure, the cells deform and successfully pass through the narrow channel.<sup>100</sup> Despite the presence of the bypass, the fluid pressure in the flow channel of the characterization zone remains unaffected, even when the cells squeeze through the narrow channel and temporarily block the flow.<sup>101</sup> During the passage through the first narrow channel, the external force remains relatively constant, and the passage time exhibits an inverse correlation with the cell's deformation ability. Therefore, by quantifying the passage time, it is possible to compare and measure the deformation ability and elastic modulus of different groups of cells. The QDC method offers an improved approach for high-throughput quantification of cell viscoelasticity. Recent studies have indicated that cancer cells possess softer mechanical properties compared to normal cells, as demonstrated by smaller deformation parameters in QDC tests.<sup>102</sup>

### 3.2.7. Micropipette aspiration

Micropipette aspiration (MA) is a cost-effective technique widely used in the study of deformation mechanics in whole cell or vesicle membranes.<sup>103</sup> In MA experiments, membranes are pulled into a glass tube of known inner diameter, usually with a micropipette smaller than the vesicle diameter, using a vacuum. The membrane then slides and deforms inside the tube under continuous suction. Previous studies have observed various regimes of bending and membrane surface area expansion over extended periods of time.<sup>25</sup> In the bent state, the lipid bilayer acts as an incompressible material, preserving the total membrane area. However, in the area expansion regime with higher tension, the membrane experiences strain due to the direct expansion of the surface area of each lipid molecule. The applied suction pressure typically falls within the range of 0.1–1 kPa, and measurement resolutions as precise as  $\pm 25$  nm have been reported. Estimating the force on the vesicle requires knowledge of the pressure difference. Various experiments have been conducted using MA to investigate the viscoelastic behavior and volumetric strain of erythrocytes, cytoskeletal actin, and chondrocytes. Recently, Bhatia et al.<sup>104</sup> employed MA to characterize giant unilamellar vesicles (GUVs) featuring embedded nanotubes on their membrane surface. Although these GUVs lack internal structures like cytoskeletons or organelles, they exhibit behavior similar to cell membranes due to the increased elasticity bestowed by the embedded nanotubes. In general, MA is capable of monitoring dynamic changes in cell membrane properties following treatment with agents such as drugs. For example, Lee et al. employed MA to assess the stiffening of breast cancer cells (MDA-MB-231) after introducing Taxol. MA can be readily adapted to a microfluidic setup compared to other techniques, largely due to its minimal hardware requirements. However, its usefulness in measuring larger vesicles is limited by the physical size of the pipette.<sup>105</sup>

### 3.2.8. Brillouin microscopy

Confocal Brillouin microscopy (BM) was proposed as a nondestructive, label- and contact-free technique in 2008, which allows probing of mechanical properties in a high resolution. On the basis of visible or infrared monochromatic (laser) light from gigahertz-frequency longitudinal acoustic phonons to acquire the resulting Brillouin spectrum, it is capable of gaining the information of the longitudinal modulus of the (bio-)material. Coupled to a confocal microscope, BM is enabled to achieve diffraction-limited resolution in 3D. Therefore, BM was widely applied in the research of intracellular biomechanics in living cells, ex vivo and in vivo tissues and biomaterials as well as the diseases diagnosis.

Meanwhile, in order to overcome the problem of the weak typical signal levels and difficulty in achieving high resolution, stimulated Brillouin scattering (SBS) was introduced to acquire high mechanical specificity. Through the coherently driving, and thus enhancing, the phonon population inside a sample at a given frequency via two interfering laser (pump) beam, SBS is capable of spectral measurements at a higher resolution that are free of elastic background contributions. Nevertheless, SBS is normally restricted to relatively non-absorbing samples thinner than  $\sim 100$ – $200$   $\mu\text{m}$  that can be optically accessed from two opposing sides, which constrains its development in biological sciences. To solve this flaw, a pulsed pump–probe approach was introduced, which eventually realize a substantially ( $>10$ -fold) lower illumination dosage at comparable signal-to-noise ratio (SNR), spectral resolution, image quality and speed compared to recent SBS demonstrations. This achieves photography without sample heating or phototoxic effects.<sup>106</sup>

## 4. Correlation between the ECM and cell viscoelasticity

### 4.1. Effects of ECM viscoelasticity on cell behavior

#### 4.1.1. Cell spreading and cell migration

The viscoelasticity of the ECM significantly impacts cell spreading and migration (Fig. 4a). Initially, Mooney's group focused on investigating the influence of the viscoelastic properties of the extracellular microenvironment on cell proliferation and spreading in 2D cell culture systems. To accomplish this, they developed a range of RGD-modified alginate hydrogel substrates with different initial elastic moduli, ranging from 2.8 kPa to 49.5 kPa, each with distinct relaxation rates from 79 to 519 s. Through the cultivation of C2C12 myoblasts on these substrates, they observed that only cells grown on soft RGD-modified alginate hydrogel substrates (particularly those with elastic moduli of 2.8 and 12.2 kPa) demonstrated increased cell spreading on viscoelastic substrates compared to those on elastic substrates of the same stiffness. However, no noticeable difference in cell spreading was observed on stiff substrates (Fig. 4b) (specifically, those with a modulus of 49.5 kPa).<sup>18</sup> The effects of viscoelastic substrates with low elasticity were probably mediated, at least in part, through the same pathway associated with stiffness, involving  $\beta 1$  integrin adhesions, actin polymerization, actomyosin contractility, and nuclear translocation of YAP. It is important to note that Janmey et al. observed contrasting cell spreading behaviors in normal hepatocytes (such as primary human hepatocytes, PHH) and hepatocellular carcinoma cells (such as Huh7 cells) on viscoelastic polyacrylamide substrates. They found that Huh7 cells exhibited a faster rate of cell spreading on viscoelastic substrates compared to purely elastic substrates, whereas PHH cells displayed the opposite behavior. This observation suggests that the impact of viscoelasticity on cell spreading is not static and varies depending on the cell type. According to the motor-clutch model, Huh7 cells were in a “frictional slippage” regime, and restricted retrograde flow resulted in increased cell spreading on viscoelastic substrates. In contrast, PHH cells were in a “load and fail” regime, and high retrograde flow led to decreased cell spreading on viscoelastic substrates.<sup>107</sup> Recently, studies on matrix viscoelasticity-regulated cell spreading and proliferation in 3D cell cultures have been conducted. Mooney's group developed alginate-PEG hydrogel with varying PEG density, enabling controllable regulation of stress relaxation for 3D culture,<sup>34</sup> while the stress relaxation half-times varied from tens of seconds to thousands of seconds. The study examined the effect of PEG spacer densities on stress relaxation and cell behavior of 3T3 fibroblasts encapsulated within alginate gels. The results revealed that faster stress relaxation in alginate-PEG hydrogels promoted cell spreading in 3D culture. This could be attributed to the co-localization of paxillin and  $\beta 1$ -integrin at the cell periphery, which initiated the formation of focal adhesions and enhanced cellular capacity for extracellular matrix (ECM) remodeling through nuclear localization of YAP/TAZ. The study also suggested a potential role of the nucleus in mechanotransduction towards the viscoelastic cell microenvironment, as

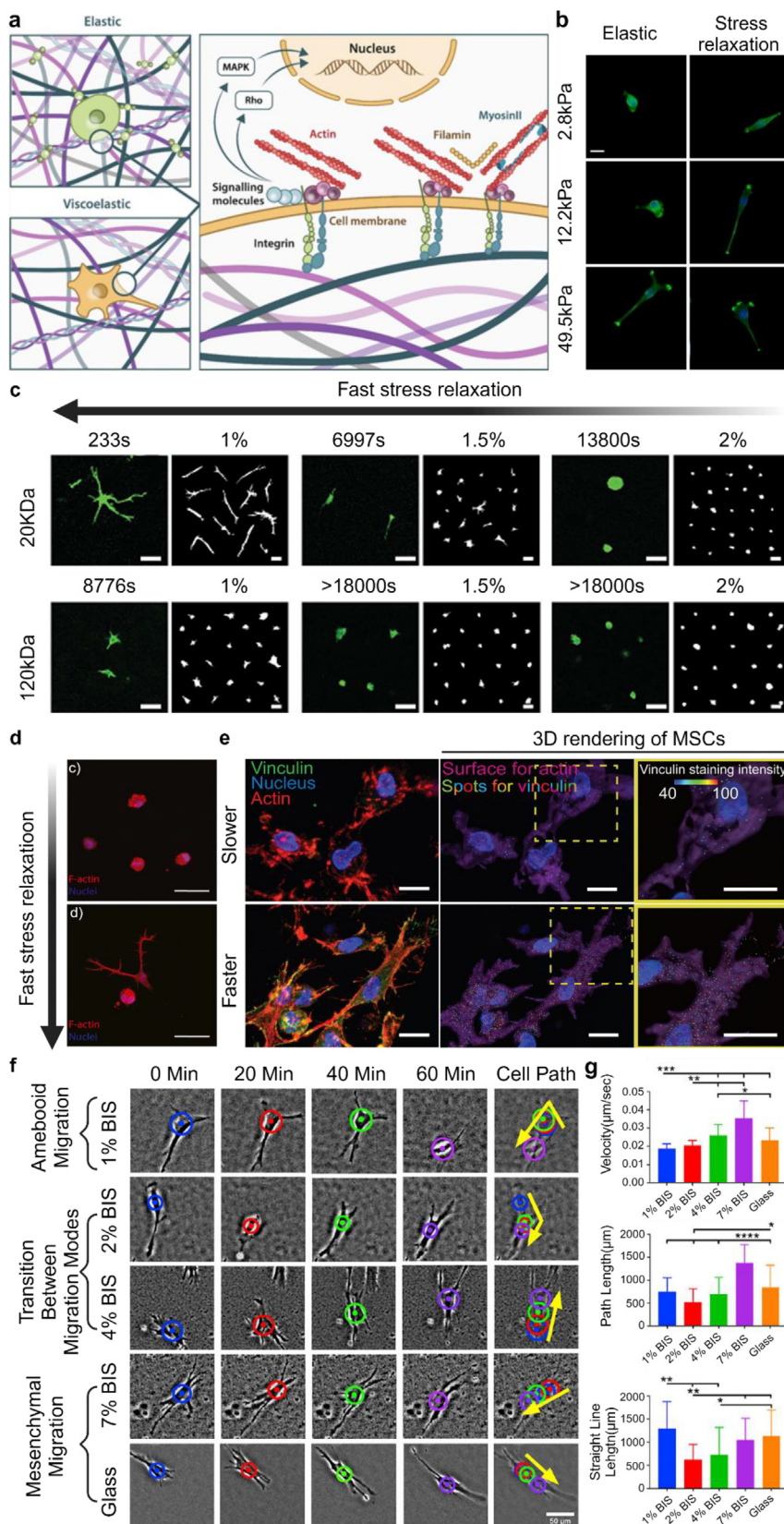


**Fig. 4.** Effect of ECM viscoelasticity on cell spreading and migration. **a)** Diagram of how cell spreading is affected by ECM viscoelasticity. **(b)** Illustrations of C2C12 cells cultured for 22 h on elastic and stress-relaxing hydrogels with initial moduli of 2.8, 12.2, and 49.5 kPa. The scale bar represents 20 micro-meters in each panel. Reproduced with permission.<sup>18</sup> **(c)** Representative images of human mesenchymal stem cells cultured in HA collagen hydrogels with tunable viscoelasticity. The right panels show MSC outlines representative of each group. The scale bar represents 50 micro-meters in each panel. Reproduced with permission.<sup>35</sup> **(d)** Representative images of hMSCs cultured in non-thioester and thioester hydrogels for 3 d. Scale bar: 50 μm. Reproduced with permission.<sup>52</sup> **(e)** Illustrations of MSC cells cultured on slower and faster stress-relaxing hydrogels. Reproduced with permission.<sup>109</sup> **(f)** Representative images of single cells migrating using either amoeboid or mesenchymal cell migration over 60 min were shown. Circles represent the cell body, while the dots represent the centroid of the cell body. Yellow arrows represent direction and relative path of migration. **(g)** quantification of cellular migration responses including velocity, path length and straight-line length. \* $p < 0.05$ ; \*\* $p < 0.01$ ; \*\*\* $p < 0.001$ ; \*\*\*\* $p < 0.0001$ . **(f-g)** Reproduced with permission.<sup>111</sup>

changes in cell spreading and YAP/TAZ distribution correlated with alterations in nuclear volume and shape. Similar findings were observed in chondrocytes<sup>108</sup> and MSCs<sup>35,52,109</sup> cultured on hydrogels with faster viscoelastic stress relaxation (Fig. 4c–e).

Cell migration is a crucial process for the establishment and maintenance of cellular functions. The microenvironment provides mechanical cues that regulate cell migration. A previous study found that liver sinusoidal endothelial cells (LSECs) cultured on polyethylene glycol (PEG)



hydrogel substrates with stiffness ranging from 140 to 610 Pa promoted collective migration of LSECs and the formation of capillary-like structures.<sup>110</sup> Recent research has focused on the influence of substrate viscoelasticity on cell migration. For example, epithelial monolayers exhibited rapid and coordinated movement on viscoelastic polyacrylamide substrates through the reorganization of both cell–matrix and cell–cell adhesions.<sup>111</sup> During this process, vinculin was transferred from focal adhesions to intercellular junctions through the cadherin complex. Along with fibronectin reorganization and focal adhesion kinase (FAK)-mediated actomyosin contractility, vinculin translocation effectively facilitated coordinated movement of epithelial monolayers (Fig. 4f and g).

In addition to substrate viscoelasticity, the viscous component of the substrate also influences the modes of cell migration. Brown's group reported that the viscoelastic properties of microgel thin films efficiently controlled migration modes in fibroblasts. On thin films with the highest loss tangent value (e.g., 1% BIS films), round or ellipsoid fibroblasts loosely attached to the substrate with poor stress fiber formation. These cells exhibited slow rates of migration and decreased spreading area, suggesting an occurrence of amoeboid cell migration. On the other hand, thin films with the lowest loss tangent value allowed elongated fibroblasts with robust stress fibers to form strong substrate adhesions, indicating a dominant mesenchymal migration. On films with intermediate loss tangent values, a transition between amoeboid and mesenchymal

migration was observed. It was confirmed that the signaling pathways mediated by ROCK and CDC42 were important in regulating amoeboid migration of fibroblasts on low loss tangent films, while the Rac pathway played a critical role in guiding mesenchymal migration of fibroblasts on films with high loss tangent values.<sup>112</sup>

#### 4.1.2. Cell differentiation and maintenance of stemness

The viscoelasticity of the ECM can influence cell differentiation (Fig. 5a). Previously, Chaudhuri's research group examined the effects of manipulating the viscoelastic properties of alginate and alginate-PEG hydrogels on mesenchymal stem cells (MSCs). They achieved this by altering the molecular weight of alginate and varying the density of the PEG spacer. The findings showed that MSCs in alginate hydrogels with faster relaxation exhibited higher levels of alkaline phosphatase (ALP) and collagen-1 expressions, as well as greater mineral formation. Similarly, in alginate-PEG hydrogels with faster stress relaxation, MSCs demonstrated increased expressions of osteogenesis markers (OCN, ALP, RUNX2, and BSP) and higher ALP activity,<sup>34</sup> suggesting enhanced osteogenic differentiation in a viscoelastic microenvironment with a fast relaxation rate (Fig. 5b and c). The study also revealed that the degree of matrix remodeling governed the osteogenesis of MSCs in a viscoelastic microenvironment. A faster relaxation rate led to greater mechanical remodeling of the matrix, resulting in improved cell spreading and MSC osteogenesis.

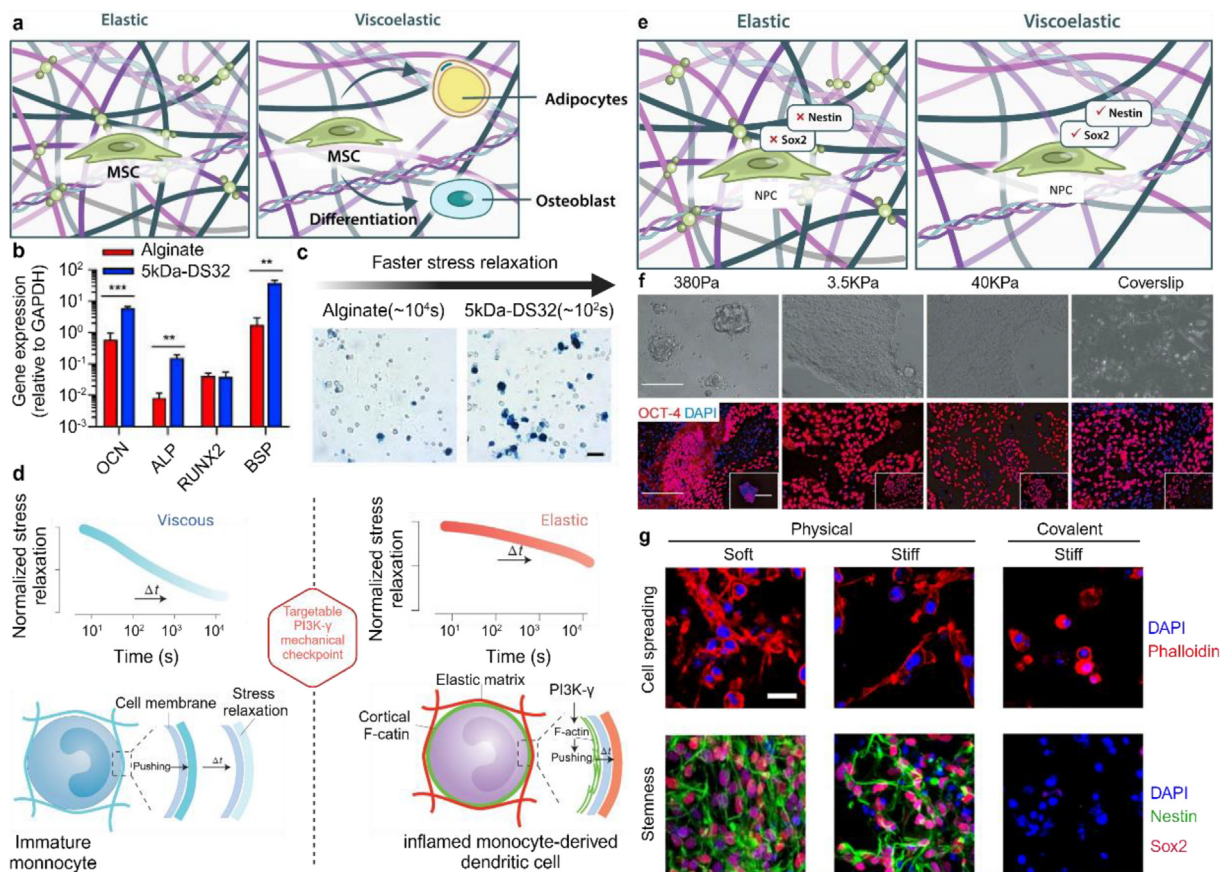


**Fig. 5.** Effect of ECM viscoelasticity on cell differentiation and maintenance of Stemness. a) Schematic diagram of the effect of ECM viscoelasticity on cell differentiation. b) Faster stress relaxation alginate-PEG hydrogels promoted osteogenic differentiation of MSCs. The gene expression of markers of osteogenesis including OCN, ALP, RUNX2, and BSP. Reproduced with permission. c) Representative images of ALP staining of MSCs in hydrogels with different stress relaxation. Scale bar: 25  $\mu$ m \*\*p < 0.01, \*\*\*p < 0.001. b-c) Reproduced with permission.<sup>34</sup> d) mechanical checkpoint of monocyte cell fate transduces external mechanical resistance to promote dendritic cell differentiation. Reproduced with permission.<sup>114</sup> e) Representative images illustrate the immunofluorescence staining of actin, nestin, sox2, and the nucleus in a viscoelastic and mechanically crosslinked alginate hydrogel as well as elastic and covalently crosslinked alginate hydrogels. f) Brightfield and immunostaining images of OCT-4 using hESCs cultured on substrates of different stiffness for five days. The scale bar represents 200 micro-meters in each panel. Reproduced with permission.<sup>119</sup> g) immunostaining images of OCT-4 using hESCs cultured on substrates of different stiffness for five days. The scale bar represents 200 micro-meters in each panel. Reproduced with permission.<sup>120</sup>

Subsequently, Chaudhuri's group further investigated how matrix remodeling affected MSC osteogenesis in viscoelastic microenvironments.<sup>113</sup> They discovered that MSCs cultured in faster-relaxing hydrogels exhibited significant volumetric expansion during cell spreading. This greater volume expansion was found to enhance osteogenic differentiation, independent of cell morphology. The study revealed a strong correlation between volume expansion, TRPV4 expression and activation, and the feedback between TRPV4 and volume expansion that increased nuclear localization of RUNX2 for facilitating MSC osteogenic differentiation. These findings emphasized the importance of stress relaxation as a crucial design parameter for biomaterials in regulating cell differentiation. This understanding can greatly contribute to stem cell-based therapy, tissue engineering, and regenerative medicine (Fig. 5d).<sup>114</sup>

Maintaining the stemness of stem cells is essential in many biomedical applications. To achieve this, stem cells must continually express proteins characteristic of the stem cell state, undergo self-renewing proliferation, and retain the capacity for appropriate differentiation into mature cell types.<sup>115</sup> Various niche factors, such as matrix stiffness, composition, and microstructure, have been shown to regulate stemness in different types of stem cells (Fig. 5e) (e.g., pluripotent stem cells, hematopoietic stem cells, MSCs, intestinal stem cells, and muscle stem cells).<sup>116–118</sup> For example, a previous study investigated the influence of substrate stiffness on embryonic stem cells and their derived progenitor cells using PEGDA hydrogels with controlled stiffness (i.e., 380 Pa, 3.5 kPa, and 40 kPa). The findings revealed that these cell types exhibited different changes in apparent Young's modulus in response to substrate stiffness, which significantly affected their maintenance of pluripotency and lineage-specific characteristics. On substrates that were too rigid or too soft, fluctuations in apparent Young's modulus occurred during cell passaging and proliferation, resulting in a loss of lineage specificity. On substrates with an "optimal" stiffness, the apparent Young's modulus remained constant, preserving lineage specificity. The effect of substrate stiffness on apparent Young's modulus and downstream cell fate was correlated with intracellular cytoskeletal organization and nuclear/cytoplasmic localization of YAP (Fig. 5f).<sup>119</sup>

Additionally, Heilshorn et al. reported that the maintenance of stemness in neural progenitor cells (NPCs) within alginate hydrogels depended on matrix viscoelasticity, regardless of the initial stiffness (Fig. 5g).<sup>120</sup> Viscoelastic and physically crosslinked alginate hydrogels facilitated matrix remodeling, cell spreading, and cell–cell contact, thereby preserving the Sox2 and Nestin expressions of NPCs at different stiffness levels. In contrast, elastic hydrogels with covalent crosslinking inhibited matrix remodeling and cell spreading, resulting in the loss of stemness. This matrix remodeling-dependent maintenance of NPC stemness in viscoelastic hydrogels occurred through modulation of cadherin-mediated  $\beta$ -catenin signaling. Utilizing a viscoelastic cell microenvironment for maintaining stemness could have broad applications in regenerative treatments following oriented differentiation.

#### 4.1.3. Cell behavior and function in diseases

The mechanical characteristics of the extracellular matrix (ECM) are crucial factors affecting cell behavior and function. They provide physical support and transmit mechanical signals that regulate biological processes within cells. These mechanical cues play a pivotal role in various diseases, notably in pathological conditions such as calcification, fibrosis, and bone-related disorders. In this part, we integrate relevant literature exploring how ECM mechanical properties influence cell behavior and function in disease contexts.

Ye et al. investigated the role of ECM mechanical properties, such as stiffness and elasticity, in regulation of lysosomal stability and cellular calcification processes, thereby influencing osteoarthritis progression. This suggests that changes in ECM mechanics could alter the cellular environment, contributing to observed pathological changes in osteoarthritis.<sup>121</sup> In another study, Zhu et al. examined fibrocytes' involvement in fibrous epulis pathogenesis. As primary producers of ECM, fibrocytes

are significantly affected by ECM mechanical properties. The stiffness of the ECM in fibrous epulis may regulate fibrocyte differentiation and migration. This underscores how ECM mechanics dictate cellular behavior in fibrotic conditions.<sup>122</sup> Moreover, Xu et al. demonstrated that a fibrotic matrix induces mesenchymal transformation of epithelial cells in oral submucous fibrosis. This transformation correlates with ECM stiffening, indicating the critical role of ECM mechanical properties in disease progression. These findings suggest that ECM stiffness drives pathological epithelial–mesenchymal transition, contributing to oral tissue fibrosis.<sup>123</sup> Additionally, Wan et al. observed that upregulation of mitochondrial dynamics promotes osteogenic differentiation of mesenchymal stem cells (MSCs) cultured on self-mineralized collagen membranes. This highlights how ECM mineralization and mechanical properties regulate intracellular mitochondrial function, thereby directing stem cell fate and supporting osteogenesis.<sup>124</sup> Furthermore, Li et al. explored the impact of matrix stiffening on guided bone regeneration, revealing that ECM stiffening enhances osteogenic differentiation through mechanical signaling pathways. This emphasizes how ECM mechanical properties are critical in bone regeneration and repair, suggesting that adjusting ECM stiffness could facilitate stem cell-mediated bone formation.<sup>125</sup> Overall, ECM mechanical properties profoundly impact cell behavior and function across diverse diseases. Mechanical signals regulate crucial cellular processes such as differentiation, migration, proliferation, and survival. Understanding and manipulating ECM mechanics offer promising therapeutic strategies for disease treatment and advancements in regenerative medicine.

#### 4.1.4. Cellular transcriptional activation

The ECM plays a crucial role in regulating various cellular processes, including gene expression. Its viscoelastic properties, encompassing both viscosity and elasticity, significantly influence how cells sense and respond to their microenvironment, ultimately impacting gene expression patterns. This intricate interplay involves a multitude of signaling pathways, each contributing to the diverse effects of ECM viscoelasticity on cellular behavior.<sup>36,126</sup>

Embedded within the cell membrane, mechanosensitive ion channels act as gatekeepers, translating mechanical forces exerted by the ECM into biochemical signals. Among these channels, Piezo1 and TRPV4 exhibit pivotal role in mediating ECM-driven gene expression changes. Piezo1-mediated calcium signaling has been shown to regulate the expression of genes involved in various cellular processes, including proliferation, differentiation, and migration.<sup>127,128</sup> For example, Piezo1 activation has been shown to promote the expression of genes associated with osteoblast differentiation and bone formation.<sup>129</sup> It has been also shown to promote cell spreading and adhesion on stiff substrates.<sup>130</sup> TRPV4-mediated calcium signaling has been implicated in the regulation of genes involved in inflammation, pain, and vascular tone.<sup>131,132</sup> For example, TRPV4 activation can promote the expression of pro-inflammatory cytokines and contribute to the development of chronic pain.<sup>133</sup> TRPV4 activation can also influence cellular behavior, such as promoting cell migration and vascular permeability.<sup>134</sup>

Integrins, transmembrane receptors with a dual role, bind to specific ECM components while simultaneously sensing the stiffness and elasticity of the surrounding matrix. This ability to translate physical cues into biochemical signals makes integrins crucial players in ECM-mediated regulation of gene expression.<sup>135</sup> Upon activation, integrins trigger various signaling pathways, including the MAPK and Rho/ROCK pathways. These pathways, in turn, regulate the activity of transcription factors, ultimately influencing gene expression patterns.<sup>136</sup> For instance, integrin-mediated signaling has been shown to regulate the expression of genes involved in cell proliferation, migration, and differentiation, highlighting its role in diverse cellular processes.<sup>137–139</sup>

The mechanisms by which ECM viscoelasticity influences gene expression extend beyond the well-characterized pathways mentioned above. Other signaling pathways, such as the YAP/TAZ pathway and the Hippo pathway, have also emerged as key players in mediating these



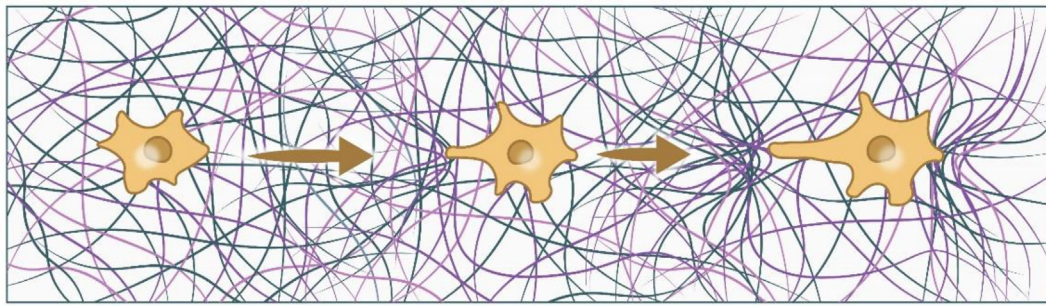


**Fig. 6.** Effect of cell contraction on ECM stress-stiffening. Cell stiffens their surrounding ECM when being encapsulated in 3D ECM systems.

effects. The YAP/TAZ pathway, primarily regulated by cell–cell contact and ECM mechanical properties, controls organ size and tissue regeneration.<sup>140</sup> In response to increased ECM viscoelasticity, YAP/TAZ translocate to the nucleus, where they interact with transcription factors and influence gene expression patterns. This pathway plays a crucial role in various processes, including tissue development, regeneration, and cancer progression.<sup>141</sup> The Hippo pathway, acting as a tumor suppressor pathway, regulates cell proliferation and apoptosis. This pathway is also sensitive to ECM mechanical properties, with increased viscoelasticity leading to the activation of the Hippo pathway and subsequent inhibition of YAP/TAZ activity.<sup>142</sup> This intricate interplay between the YAP/TAZ and Hippo pathways highlights the complex signaling landscape underlying ECM-mediated gene expression regulation.

The influence of ECM viscoelasticity on gene expression is a complex and multifaceted phenomenon, orchestrated by a symphony of signaling pathways. Mechanosensitive ion channels, integrins, and other signaling pathways work in concert to translate the physical cues of the ECM into biochemical signals, ultimately shaping the cellular response and

influencing gene expression patterns. Understanding these intricate mechanisms is crucial for unraveling the diverse roles of ECM viscoelasticity in various physiological and pathological processes, paving the way for novel therapeutic strategies targeting ECM-mediated signaling pathways.

#### 4.2. Effects of cell mechanics on ECM

##### 4.2.1. Effect of cell contraction on stress-stiffening of ECM

Although numerous prior studies have demonstrated the significant impact of the mechanical properties of the extracellular matrix (ECM) on cell behavior and function, the influence of cellular mechanical properties on the ECM remains largely unexplored. By using nonlinear stress inference microscopy (NSIM), a technique to infer stress fields in a 3D matrix from nonlinear microrheology measurements with optical tweezers, recent research has shown that cells can actively contract and thereby increase the stiffness of the surrounding ECM when encapsulated in 3D ECM systems such as collagen, fibrin, and Matrigel (Fig. 6). These forces result in spatially varied gradients of matrix stiffness induced by

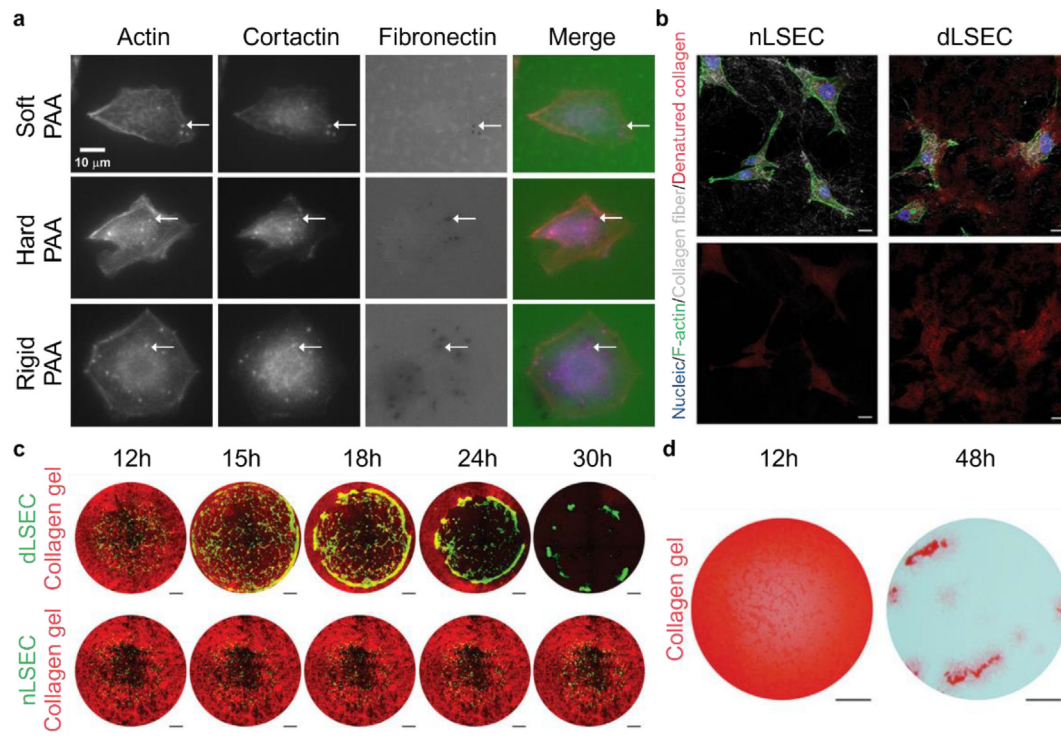


**Fig. 7.** Effect of cell stiffness on ECM remodeling and degradation. a) Invadopodia-associated ECM degradation by SCC-61 cells on PAAs. Reproduced with permission.<sup>144</sup> b) Ponceau S staining of collagen matrix after 12 and 48 h' degradation mediated by dLSECs. c) Representative fluorescent images of CHP staining of collagen matrix with degradation mediated by nLSECs and dLSECs. d) Representative images of dynamic degradation of collagen matrix mediated by nLSEC and dLSEC. b-d) Reproduced with permission.<sup>145</sup>

cells, which could serve as mediators of mechanical communication between cells.<sup>143</sup>

#### 4.2.2. Effect of cell stiffness on ECM degradation

Cells can sense the mechanical properties of the ECM through intracellular tension generated by actomyosin contractility. These contractile forces are transmitted to the surface of the matrix as traction stresses, facilitating mechanical interactions with the ECM. Researchers have recently examined the invasiveness and contractility of invasive cancer cell lines using polyacrylamide gels of varying stiffness. The experiments demonstrated that cell traction forces regulate ECM degradation, suggesting that the generation of cellular forces plays a significant role in mediating degradation of the tumor microenvironment (Fig. 7a).<sup>144</sup> Recent study also showed when compared to the normal endothelial cells, ECM-degrading liver sinusoidal endothelial cells primed by PMA and Accutase, which may have different cell viscoelasticity, exhibit superior ability to degrade collagen (Fig. 7b-d).<sup>145</sup>

## 5. Conclusion

Tissues are comprised of cells, extracellular matrix (ECM), and extracellular fluid. Recent studies have revealed the prevalence of viscoelastic properties in most tissues, which are attributed to both ECM and cell components. Viscoelasticity in ECM results from stress relaxation and creep behavior due to weak bonds between the fibrin network and attached macromolecules, while cells exhibit viscoelasticity primarily due to their high water content and cytoskeleton. This property is significant in biogenesis processes, influencing cell differentiation and activities. Various experimental techniques, such as magnetic tweezers, micropipette aspiration, and atomic force microscopy, are used to investigate the viscoelastic properties of materials and cells, but inconsistencies in measurement modes and parameters limit the comparability of results, necessitating the standardization of these methods. Recent research highlights the role of viscoelasticity in regulating cell behavior and its impact on ECM component and structure, influencing tissue development and disease. The future development of the field is to summarize and standardize the testing methods for ECM and cell viscoelasticity to enhance comparability and advance the fields of tissue engineering and regenerative medicine.

## 6. Outlook

With the rapid advance of biomechanics, there is increasing evidence that highlights the significance of viscoelasticity as a fundamental mechanical characteristic of living organisms. While the recent advancements in this rapidly evolving field have shed light on the correlation between cell viscoelasticity and ECM, the influence of cell physical properties on the ECM remains an area that requires further investigation. The specific mechanisms through which cell physical properties, such as cell stiffness or contractility, affect the ECM are not yet fully understood. This article provides a comprehensive overview of the recent advancements in this rapidly evolving field. It also examines the challenges faced and potential directions to explore, including the origin, measurement methods, and correlations between extracellular matrix (ECM) and cell viscoelasticity. Moving forward, this review identifies three major areas that warrant further improvement in this field: the development of novel experimental techniques, the establishment of standardized measurement methods, and the customization of viscoelasticity.

### 6.1. Effects of cell mechanics on ECM

Compared to the influence of the physical properties of the extracellular matrix on cell behavior and function, the influence of cell physical properties on the extracellular matrix has yet to be thoroughly investigated. Future research should focus on understanding the impact

of cell viscoelasticity on the degradation, reorganization, and sedimentation of the extracellular matrix, particularly in relation to the ECM's degradation and reorganization. Furthermore, exploring the interaction between the viscoelasticity of the extracellular matrix and cells and its potential applications in biology and medicine is essential.

### 6.2. New tools for viscoelasticity measurement

In recent years, numerous experimental techniques have been employed to investigate the viscoelasticity of the extracellular matrix (ECM) and cells. These methods include utilizing a dynamic rheometer to measure the viscoelasticity of the ECM, as well as employing techniques such as nuclear magnetic resonance (NMR), ultrasound, atomic force microscopy (AFM), optical tweezers, and micropipette aspiration to measure the viscoelasticity of cells. However, a common limitation of these traditional methods is the relatively small number of samples that can be measured within a reasonable time frame. The throughput of measuring only dozens or even hundreds of samples per hour is incomparable to the high-throughput sequencing and flow analysis used in biological experiments. Fortunately, microfluidic-based experimental methods have emerged as a promising approach to greatly enhance the efficiency of measuring the viscoelasticity of cell samples. These microfluidic techniques have the potential to accomplish high-throughput screening. Additionally, another avenue for improving experimental throughput is the integration of high-throughput data collection with artificial intelligence analysis. This integration would enable making AI predictions based on ample data.

### 6.3. Standardization of measurement methods

One of the key factors that significantly impacts the widespread application of biomechanics in biology and medicine is the lack of standardized protocols. The differences in measurement modes among various methods, such as the size of the measurement area and the application of force, result in vastly different experimental outcomes, even when measuring the same sample. Traditionally, there have been orders of magnitude discrepancies in results, highlighting the crucial need for standardized experimental procedures and methods in biomechanical measurements. A potential solution could be the use of standardized, inert bionic materials as reference samples. For example, when doing a cell assay, GUV can be measured as a standard sample to calibrate the differences between measurement tools.<sup>146</sup> By including reference samples in all types of experiments, a consistent benchmark can be established for comparative analysis. Furthermore, inspired by the formation process of databases like genomes, proteomes, and transcriptomes, the development of a high-throughput technology-based biomechanical database with standardized protocols holds promise for the future.

### 6.4. Tailor viscoelasticity for therapy

The time scale is a crucial factor in biological processes within the body. While certain processes like signal transduction and cell activation occur rapidly, others, such as stem cell differentiation, can span tens of days. Hence, future developments in viscoelastic material design must consider a broader time scale to match physiological conditions. Additionally, it is essential to investigate the precise control of material and cell viscoelasticity. This can be achieved through the development of biomaterials with adjustable viscoelastic properties, thereby combining the viscoelasticity of biomaterials with cell viscoelasticity to achieve temporal precision. Regulating the viscoelasticity allows cells to alter their physiological functions by becoming softer or stiffer under different conditions, providing a new avenue for further exploration. In the context of biological therapy, these developments are significant. By creating biomaterials with tunable viscoelastic properties, we can better mimic physiological conditions, thereby promoting stem cell

differentiation and tissue regeneration. This approach holds promise for regenerative medicine, providing new therapeutic strategies. Moreover, precise control of cell viscoelasticity could have broader biomedical applications, such as in drug screening and disease diagnostics.

## Ethical approval

This study does not contain any studies with human or animal subjects performed by any of the authors.

## CRediT authorship contribution statement

**Zhiqiang Liu:** Investigation, Methodology, Supervision, Validation, Writing – original draft. **Si Da Ling:** Writing – original draft. **Kaini Liang:** Visualization, Writing – original draft. **Yihan Chen:** Visualization, Writing – original draft. **Yudi Niu:** Validation, Writing – original draft. **Lei Sun:** Visualization, Writing – review & editing. **Junyang Li:** Writing – original draft. **Yanan Du:** Resources, Supervision, Validation, Writing – original draft, Writing – review & editing.

## Declaration of competing interest

The authors declare that they have no known competing financial interests or personal relationships that could have appeared to influence the work reported in this paper.

## Acknowledgments

We apologize to those authors whose work we were unable to cite because of space constraints. This work was financially supported by the National Natural Science Foundation of China (grant no. 82061148010). Parts of figures were created with BioRender (BioRender.com).

## References

- Sotres J, Jankovskaja S, Wannerberger K, Arnebrant T. Ex-vivo force spectroscopy of intestinal mucosa reveals the mechanical properties of mucus blankets. *Sci Rep.* 2017;7:7270.
- Rho JY, Ashman RB, Turner CH. Young's modulus of trabecular and cortical bone material: ultrasonic and microtensile measurements. *J Biomech.* 1993;26:111–119.
- McKinnon DD, Domaille DW, Cha JN, Anseth KS. Biophysically defined and cytocompatible covalently adaptable networks as viscoelastic 3D cell culture systems. *Adv Mater.* 2014;26:865–872.
- Qiu S, Zhao X, Chen J, et al. Characterizing viscoelastic properties of breast cancer tissue in a mouse model using indentation. *J Biomech.* 2018;69:81–89.
- Geerlings M, Peters GWM, Ackermans PAJ, Oomens CWJ, Baaijens FPT. Linear viscoelastic behavior of subcutaneous adipose tissue. *Biorheology.* 2008;45:677–688.
- Pereplyuk M, Chin L, Cao X, et al. Normal and fibrotic rat livers demonstrate shear strain softening and compression stiffening: a model for soft tissue mechanics. *PLoS ONE.* 2016;11:e0146588.
- Liu Z, Bilston L. On the viscoelastic character of liver tissue: experiments and modelling of the linear behaviour. *Biorheology.* 2000;37:191–201.
- Reihnsner R, Menzel EJ. Two-dimensional stress-relaxation behavior of human skin as influenced by non-enzymatic glycation and the inhibitory agent aminoguanidine. *J Biomech.* 1998;31:985–993.
- Abdel-Wahab AA, Alam K, Silberschmidt VV. Analysis of anisotropic viscoelastoplastic properties of cortical bone tissues. *J Mech Behav Biomed Mater.* 2011;4:807–820.
- Connizzo BK, Grodzinsky AJ. Multiscale poroviscoelastic compressive properties of mouse supraspinatus tendons are altered in Young and aged mice. *J Biomech Eng.* 2018;140:051002.
- Troyer KL, Puttlitz CM. Human cervical spine ligaments exhibit fully nonlinear viscoelastic behavior. *Acta Biomater.* 2011;7:700–709.
- Coluccino L, Peres C, Gottardi R, Bianchini P, Diaspro A, Ceseracciu L. Anisotropy in the viscoelastic response of knee meniscus cartilage. *J Appl Biomater Funct Mater.* 2017;15:77–83.
- Nam S, Hu KH, Butte MJ, Chaudhuri O. Strain-enhanced stress relaxation impacts nonlinear elasticity in collagen gels. *Proc Natl Acad Sci U S A.* 2016;113:5492–5497.
- Münster S, Jawerth LM, Leslie BA, Weitz JI, Fabry B, Weitz DA. Strain history dependence of the nonlinear stress response of fibrin and collagen networks. *Proc Natl Acad Sci USA.* 2013;110:12197–12202.
- Bhat S, Jun D, C, B, S Dahms TE. Viscoelasticity in biological systems: a special focus on microbes. In: De Vicente J, ed. *Viscoelasticity - from Theory to Biological Applications.* InTech; 2012.
- Li W, Shepherd DET, Espino DM. Frequency dependent viscoelastic properties of porcine brain tissue. *J Mech Behav Biomed Mater.* 2020;102:103460.
- Chaudhuri O, Gu L, Klumpers D, et al. Hydrogels with tunable stress relaxation regulate stem cell fate and activity. *Nat Mater.* 2016;15:326–334.
- Bauer A, Gu L, Kwee B, et al. Hydrogel substrate stress-relaxation regulates the spreading and proliferation of mouse myoblasts. *Acta Biomater.* 2017;62:82–90.
- Crick FHC, Hughes AFW. *THE PHYSICAL PROPERTIES OF CYTOPLASM A STUDY BY MEANS OF THE MAGNETIC PARTICLE hll:THOD.* Strangeways Research Laboratory; 1949.
- Hong X, Rzeczycki PM, Keswani RK, et al. Acoustic tweezing cytometry for mechanical phenotyping of macrophages and mechanopharmaceutical cytotoxicity. *Sci Rep.* 2019;9:5702.
- Wang X, Law J, Luo M, et al. Magnetic measurement and stimulation of cellular and intracellular structures. *ACS Nano.* 2020;14:3805–3821.
- Bausch AR, Möller W, Sackmann E. Measurement of local viscoelasticity and forces in living cells by magnetic tweezers. *Biophysical J.* 1999;76:573–579.
- Bausch AR, Ziemann F, Boulbitch AA, Jacobson K, Sackmann E. Local measurements of viscoelastic parameters of adherent cell surfaces by magnetic bead microrheometry. *Biophysical J.* 1998;75:2038–2049.
- Mitchison JM, Swann MM. *The mechanical properties of the cell surface.* In: *The Mechanical Properties of the Cell Surface.* vol. 17. 1953.
- Sato M, Theret DP, Wheeler LT, Ohshima N, Nerem RM. Application of the micropipette technique to the measurement of cultured porcine aortic endothelial cell viscoelastic properties. *J Biomech Eng.* 1990;112:263–268.
- Efremov YM, Wang W-H, Hardy SD, Geahlen RL, Raman A. Measuring nanoscale viscoelastic parameters of cells directly from AFM force-displacement curves. *Sci Rep.* 2017;7:1541.
- Isaksson H, Nagao S, Malkiewicz M, Julkunen P, Nowak R, Jurvelin JS. Precision of nanoindentation protocols for measurement of viscoelasticity in cortical and trabecular bone. *J Biomech.* 2010;43:2410–2417.
- Lyubin EV. Cellular viscoelasticity probed by active rheology in optical tweezers. *J Biomed Opt.* 2012;17:101510.
- Ermilov SA, Brownell WE, Anvari B. Effect of salicylate on outer hair cell plasma membrane viscoelasticity: studies using optical tweezers. In: Cartwright AN, ed. *Volume 2: Biomedical and Biotechnology Engineering.* 2004:136. <https://doi.org/10.1117/12.529200>. San Jose, CA.
- Keese C. Substrate mechanics and cell spreading. *Exp Cell Res.* 1991;195:528–532.
- Pelham RJ. Cell locomotion and focal adhesions are regulated by substrate flexibility. *Proc Natl Acad Sci USA.* 1997;94.
- Discher DE, Janmey P, Wang Y. Tissue cells feel and respond to the stiffness of their substrate. *Science.* 2005;310:1139–1143.
- Chaudhuri O, Gu L, Darnell M, et al. Substrate stress relaxation regulates cell spreading. *Nat Commun.* 2015;6:6365.
- Nam S, Stowers R, Lou J, Xia Y, Chaudhuri O. Varying PEG density to control stress relaxation in alginate-PEG hydrogels for 3D cell culture studies. *Biomaterials.* 2019;200:15–24.
- Lou J, Stowers R, Nam S, Xia Y, Chaudhuri O. Stress relaxing hyaluronic acid-collagen hydrogels promote cell spreading, fiber remodeling, and focal adhesion formation in 3D cell culture. *Biomaterials.* 2018;154:213–222.
- Humphrey JD, Dufresne ER, Schwartz MA. Mechanotransduction and extracellular matrix homeostasis. *Nat Rev Mol Cell Biol.* 2014;15:802–812.
- Bonnans C, Chou J, Werb Z. Remodelling the extracellular matrix in development and disease. *Nat Rev Mol Cell Biol.* 2014;15:786–801.
- Sauer F, Oswald L, Ariza de Schellenberger A, et al. Collagen networks determine viscoelastic properties of connective tissues yet do not hinder diffusion of the aqueous solvent. *Soft Matter.* 2019;15:3055–3064.
- Ban E, Franklin JM, Nam S, et al. Mechanisms of plastic deformation in collagen networks induced by cellular forces. *Biophysical J.* 2018;114:450–461.
- Yang W, Sherman VR, Gludovatz B, et al. On the tear resistance of skin. *Nat Commun.* 2015;6:6649.
- Silver FH, Freeman JW, Seehra GP. Collagen self-assembly and the development of tendon mechanical properties. *J Biomech.* 2003;36:1529–1553.
- Chaudhuri O, Cooper-White J, Janmey PA, Mooney DJ, Shenoy VB. Effects of extracellular matrix viscoelasticity on cellular behaviour. *Nature.* 2020;584:535–546.
- DeBenedictis EP, Keten S. Mechanical unfolding of alpha- and beta-helical protein motifs. *Soft Matter.* 2019;15:1243–1252.
- Takahashi H, Rico F, Chipot C, Scheuring S.  $\alpha$ -Helix unwinding as force buffer in spectrins. *ACS Nano.* 2018;12:2719–2727.
- Zhao X. Multi-scale multi-mechanism design of tough hydrogels: building dissipation into stretchy networks. *Soft Matter.* 2014;10:672–687.
- Brown AEX, Litvinov RI, Discher DE, Purohit PK, Weisel JW. Multiscale mechanics of fibrin polymer: gel stretching with protein unfolding and loss of water. *Science.* 2009;325:741–744.
- Paramore S, Ayton GS, Voth GA. Extending a spectrin repeat unit. II: rupture behavior. *Biophysical J.* 2006;90:101–111.
- Parada GA, Zhao X. Ideal reversible polymer networks. *Soft Matter.* 2018;14:5186–5196.
- Charrier EE, Pogoda K, Wells RG, Janmey PA. Control of cell morphology and differentiation by substrates with independently tunable elasticity and viscous dissipation. *Nat Commun.* 2018;9:449.
- Cameron Andrew R, Frith Jessica E, Cooper-White Justin J. The influence of substrate creep on mesenchymal stem cell behaviour and phenotype. *Biomaterials.* 2011;32:5979–5993.
- Tang S, Ma H, Tu HC, Wang HR, Lin PC, Anseth KS. Adaptable fast relaxing boronate-based hydrogels for probing cell-matrix interactions. *Adv Sci.* 2018;5:1800638.



52. Brown TE, Carberry BJ, Worrell BT, et al. Photopolymerized dynamic hydrogels with tunable viscoelastic properties through thioester exchange. *Biomaterials*. 2018; 178:496–503.
53. Marozas IA, Anseth KS, Cooper-White JJ. Adaptable boronate ester hydrogels with tunable viscoelastic spectra to probe timescale dependent mechanotransduction. *Biomaterials*. 2019;223:119430.
54. Zhao X, Huebsch N, Mooney DJ, Suo Z. Stress-relaxation behavior in gels with ionic and covalent crosslinks. *J Appl Phys*. 2010;107:063509.
55. Loebel C, Mauck RL, Burdick JA. Local nascent protein deposition and remodelling guide mesenchymal stromal cell mechanosensing and fate in three-dimensional hydrogels. *Nat Mater*. 2019;18:883–891.
56. Dooling LJ, Buck ME, Zhang W-B, Tirrell DA. Programming molecular association and viscoelastic behavior in protein networks. *Adv Mater*. 2016;28:4651–4657.
57. Vining KH, Stafford A, Mooney DJ. Sequential modes of crosslinking tune viscoelasticity of cell-instructive hydrogels. *Biomaterials*. 2019;188:187–197.
58. Richardson BM, Wilcox DG, Randolph MA, Anseth KS. Hydrazine covalent adaptable networks modulate extracellular matrix deposition for cartilage tissue engineering. *Acta Biomater*. 2019;83:71–82.
59. Fletcher DA, Mullins RD. Cell mechanics and the cytoskeleton. *Nature*. 2010;463: 485–492.
60. Pegoraro AF, Janmey P, Weitz DA. Mechanical properties of the cytoskeleton and cells. *Cold Spring Harb Perspect Biol*. 2017;9:a022038.
61. Trickey WR, Vail TP, Guilak F. The role of the cytoskeleton in the viscoelastic properties of human articular chondrocytes. *J Orthop Res*. 2004;22:131–139.
62. Mollaeian K, Liu Y, Bi S, Ren J. Atomic force microscopy study revealed velocity-dependence and nonlinearity of nanoscale poroelasticity of eukaryotic cells. *J Mech Behav Biomed Mater*. 2018;78:65–73.
63. Hu J, Jafari S, Han Y, Grodzinsky AJ, Cai S, Guo M. Size- and speed-dependent mechanical behavior in living mammalian cytoplasm. *Proc Natl Acad Sci U S A*. 2017;114:9529–9534.
64. Mitchison TJ, Charras GT, Mahadevan L. Implications of a poroelastic cytoplasm for the dynamics of animal cell shape. *Seminars Cell & Dev Biol*. 2008;19: 215–223.
65. Guo M, Ehrlicher AJ, Jensen MH, et al. Probing the stochastic, motor-driven properties of the cytoplasm using force spectrum microscopy. *Cell*. 2014;158: 822–832.
66. Humphrey D, Duggan C, Saha D, Smith D. Active fluidization of polymer networks through molecular motors. *Nature*. 2002;416.
67. Corominas-Murtra B, Petridou NI. Viscoelastic networks: forming cells and tissues. *Front Physiol*. 2021;9:666916.
68. Ma Y, Han T, Yang Q, et al. Viscoelastic cell microenvironment: hydrogel-based strategy for recapitulating dynamic ECM mechanics. *Adv Funct Mater*. 2021;31: 2100848.
69. Rolley E, Snoeijer JH, Andreotti B. A flexible rheometer design to measure the visco-elastic response of soft solids over a wide range of frequency. *Rev Sci Instrum*. 2019;90:023906.
70. Yoo L, Gupta V, Lee C, Kavehpore P, Demer JL. Viscoelastic properties of bovine orbital connective tissue and fat: constitutive models. *Biomech Model Mechanobiol*. 2011;10:901–914.
71. Anssari-Benam A, Bader DL, Screen HRC. A combined experimental and modelling approach to aortic valve viscoelasticity in tensile deformation. *J Mater Sci Mater Med*. 2011;22:253–262.
72. McKee CT, Last JA, Russell P, Murphy CJ. Indentation versus tensile measurements of young's modulus for soft biological tissues. *Tissue Eng B Rev*. 2011;17:155–164.
73. Barak MM, Black MA. A novel use of 3D printing model demonstrates the effects of deteriorated trabecular bone structure on bone stiffness and strength. *J Mech Behav Biomed Mater*. 2018;78:455–464.
74. Moshtagh PR, Pouran B, Korthagen NM, Zadpoor AA, Weinans H. Guidelines for an optimized indentation protocol for measurement of cartilage stiffness: the effects of spatial variation and indentation parameters. *J Biomech*. 2016;49:3602–3607.
75. Elleuch R, Taktak W. Viscoelastic behavior of HDPE polymer using tensile and compressive loading. *J Mater Eng Perform*. 2006;15:111–116.
76. Shi Y, Glaser KJ, Venkatesh SK, Ben-Abraham EI, Ehman RL. Feasibility of using 3D MR elastography to determine pancreatic stiffness in healthy volunteers: 3D MRE of the Pancreas. *J Magn Reson Imag*. 2015;41:369–375.
77. Murphy MC, Huston 3rd J, Jack Jr CR, et al. Measuring the characteristic topography of brain stiffness with magnetic resonance elastography. *PLoS ONE*. 2013;8:e81668.
78. Sack I, Jöhrens K, Würfel J, Braun J. Structure-sensitive elastography: on the viscoelastic powerlaw behavior of in vivo human tissue in health and disease. *Soft Matter*. 2013;9:5672.
79. Anvari A, Dhyani M, Stephen AE, Samir AE. Reliability of shear-wave elastography estimates of the Young modulus of tissue in follicular thyroid neoplasms. *Am J Roentgenol*. 2016;206:609–616.
80. Crichton ML, Donose BC, Chen X, Raphael AP, Huang H, Kendall MA. The viscoelastic, hyperelastic and scale dependent behaviour of freshly excised individual skin layers. *Biomaterials*. 2011;32:4670–4681.
81. Baselt DR, Revel JP, Baladeschwieler JD. Subfibrillar structure of type I collagen observed by atomic force microscopy. *Biophysical J*. 1993;65:2644–2655.
82. Radmacher M, Fritz M, Cleveland JP, Walters DA, Hansma PK. Imaging adhesion forces and elasticity of lysozyme adsorbed on mica with the atomic force microscope. *Langmuir*. 1994;10:3809–3814.
83. Chim YH, Mason LM, Rath N, Olson MF, Tassieri M, Yin H. A one-step procedure to probe the viscoelastic properties of cells by Atomic Force Microscopy. *Sci Rep*. 2018;8:14462.
84. Grant CA, Twigg PC, Tobin DJ. Static and dynamic nanomechanical properties of human skin tissue using atomic force microscopy: effect of scarring in the upper dermis. *Acta Biomater*. 2012;8:4123–4129.
85. Robertson-Anderson RM. Optical tweezers microrheology: from the basics to advanced techniques and applications. *ACS Macro Lett*. 2018;7:968–975.
86. Optical Tweezers. *Methods and Protocols*. vol. 1486. New York, NY: Springer New York; 2017.
87. Single Molecule Analysis. *Methods and Protocols*. vol. 1665. New York, NY: Springer New York; 2018.
88. Rezaei N, Downing PBB, Wiczkorek A, et al. Using optical tweezers to study mechanical properties of collagen. In: Kashyap R, Têtu M, Kleiman RN, eds. *Volume 2: Biomedical and Biotechnology Engineering*. 2011:80070K. <https://doi.org/10.1117/12.905714>. Ottawa, Canada.
89. Staunton JR, Vieira W, Fung KL, Lake R, Devine A, Tanner K. Mechanical properties of the tumor stromal microenvironment probed in vitro and ex vivo by in situ-calibrated optical trap-based active microrheology. *Cell Mol Bieng*. 2016;9: 398–417.
90. Schmidt FrankG, Ziemann F, Sackmann E. Shear field mapping in actin networks by using magnetic tweezers. *Eur Biophys J*. 1996;24.
91. Rother J, Nöding H, Mey I, Janshoff A. Atomic force microscopy-based microrheology reveals significant differences in the viscoelastic response between malignant and benign cell lines. *Open Biol*. 2014;4:140046.
92. Alcaraz J, Buscemi L, Grabulosa M, et al. Microrheology of human lung epithelial cells measured by atomic force microscopy. *Biophysical J*. 2003;84:2071–2079.
93. Lim CT, Zhou EH, Quek ST. Mechanical models for living cells—a review. *J Biomech*. 2006;39:195–216.
94. Shin D, Athanasiou K. Cytoindentation for obtaining cell biomechanical properties. *J Orthop Res*. 1999;17:880–890.
95. Schwingel M, Bastmeyer M. Force mapping during the formation and maturation of cell adhesion sites with multiple optical tweezers. *PLoS ONE*. 2013;8:e54850.
96. Ayala YA, Pontes B, Ether DS, et al. Rheological properties of cells measured by optical tweezers. *BMC Biophys*. 2016;9:5.
97. Wilhelm C, Gazeau F, Bacri J-C. Rotational magnetic endosome microrheology: viscoelastic architecture inside living cells. *Phys Rev E*. 2003;67:061908.
98. Puig-De-Morales M, Grabulosa M, Alcaraz J, et al. Measurement of cell microrheology by magnetic twisting cytometry with frequency domain demodulation. *J Appl Physiology*. 2001;91:1152–1159.
99. Chowdhury F, Na S, Li D, et al. Material properties of the cell dictate stress-induced spreading and differentiation in embryonic stem cells. *Nat Mater*. 2010;9:82–88.
100. Nyberg KD, Hu KH, Kleinman SH, Khismatullin DB, Butte MJ, Rowat AC. Quantitative deformability cytometry: rapid, calibrated measurements of cell mechanical properties. *Biophysical J*. 2017;113:1574–1584.
101. Ling SD, Geng Y, Chen A, Du Y, Xu J. Enhanced single-cell encapsulation in microfluidic devices: from droplet generation to single-cell analysis. *Biomechanics*. 2020;14:061508.
102. Naqvi SM, Vedicherla S, Gansau J, et al. Living cell factories - electrosprayed microcapsules and microcarriers for minimally invasive delivery. *Adv Mater*. 2016; 28:5662–5671.
103. Vigmostad S, Krog B, Nauseef J, Henry M, Keshav V. Alterations in cancer cell mechanical properties after fluid shear stress exposure: a micropipette aspiration study. *Cell Health Cytoskeleton*. 2015;7:25–35.
104. Ozawa H, Matsumoto T, Ohashi T, Sato M, Kokubun S. Comparison of spinal cord gray matter and white matter softness: measurement by pipette aspiration method. *J Neurosurg Spine*. 2001;95:221–224.
105. Lee LM, Liu AP. The application of micropipette aspiration in molecular mechanics of single cells. *J Nanotechnol Eng Med*. 2014;5:040902.
106. Zhang J, Nikolic M, Tanner K, Scarcelli G. Rapid biomechanical imaging at low irradiation level via dual line-scanning Brillouin microscopy. *Nat Methods*. 2023; 20(5):677–681.
107. Mandal K, Gong Z, Rylander A, Shenoy VB, Janmey PA. Opposite responses of normal hepatocytes and hepatocellular carcinoma cells to substrate viscoelasticity. *Biomater Sci*. 2020;8:1316–1328.
108. Lee H, Gu L, Mooney DJ, Levenston ME, Chaudhuri O. Mechanical confinement regulates cartilage matrix formation by chondrocytes. *Nat Mater*. 2017;16: 1243–1251.
109. Huang D, Li Y, Ma Z, et al. Collagen hydrogel viscoelasticity regulates MSC chondrogenesis in a ROCK-dependent manner. *Sci Adv*. 2023;9:eade9497.
110. Liu L, You Z, Yu H, et al. Mechanotransduction-modulated fibrotic microniches reveal the contribution of angiogenesis in liver fibrosis. *Nat Mater*. 2017;16: 1252–1261.
111. Chester D, Kathard R, Nortey J, Nellenbach K, Brown AC. Viscoelastic properties of microgel thin films control fibroblast modes of migration and pro-fibrotic responses. *Biomaterials*. 2018;185:371–382.
112. Wisdom KM, Adebawale K, Chang J, et al. Matrix mechanical plasticity regulates cancer cell migration through confining microenvironments. *Nat Commun*. 2018;9: 4144.
113. Lee H, Stowers R, Chaudhuri O. Volume expansion and TRPV4 activation regulate stem cell fate in three-dimensional microenvironments. *Nat Commun*. 2019;10:529.
114. Mechanical checkpoint regulates monocyte differentiation in fibrotic niches. *Nat Mater*. 2022;21:939–950.
115. Engler AJ, Sen S, Sweeney HL, Discher DE. Matrix elasticity directs stem cell lineage specification. *Cell*. 2006;126:677–689.
116. Miroshnikova YA, Adebawale K, Chang J, et al. Engineering strategies to recapitulate epithelial morphogenesis within synthetic three-dimensional extracellular matrix with tunable mechanical properties. *Phys Biol*. 2011;8:026013.



117. Mao AS, Özkale B, Shah NJ, et al. Programmable microencapsulation for enhanced mesenchymal stem cell persistence and immunomodulation. *Proc Natl Acad Sci U S A*. 2019;116:15392–15397.
118. Xie J, Bao M, Hu X, Koopman WJH, Huck WTS. Energy expenditure during cell spreading influences the cellular response to matrix stiffness. *Biomaterials*. 2021; 267:120494.
119. Guo A, Wang B, Lyu C, et al. Consistent apparent Young's modulus of human embryonic stem cells and derived cell types stabilized by substrate stiffness regulation promotes lineage specificity maintenance. *Cell Regen*. 2020;9:15.
120. Madl CM, LeSavage BL, Dewi RE, et al. Maintenance of neural progenitor cell stemness in 3D hydrogels requires matrix remodelling. *Nat Mater*. 2017;16:1233–1242.
121. Ye T, Wang C, Yan J, et al. Lysosomal destabilization: a missing link between pathological calcification and osteoarthritis. *Bioact Mater*. 2024;34:37–50.
122. Zhu Y, Wan MC, Gao P, et al. Fibrocyte: a missing piece in the pathogenesis of fibrous epulis. ; 2023. <https://doi.org/10.21203/rs.3.rs-2458647/v1>.
123. Xu H-Q, Guo ZX, Yan JF, et al. Fibrotic matrix induces mesenchymal transformation of epithelial cells in oral submucous fibrosis. *Am J Pathology*. 2023;193:1208–1222.
124. Wan M-C, Tang XY, Li J, et al. Upregulation of mitochondrial dynamics is responsible for osteogenic differentiation of mesenchymal stem cells cultured on self-mineralized collagen membranes. *Acta Biomater*. 2021;136:137–146.
125. Li J, Yan JF, Wan QQ, et al. Matrix stiffening by self-mineralizable guided bone regeneration. *Acta Biomater*. 2021;125:112–125.
126. Wang N, Tytell JD, Ingber DE. Mechanotransduction at a distance: mechanically coupling the extracellular matrix with the nucleus. *Nat Rev Mol Cell Biol*. 2009;10:75–82.
127. Coste B, Mathur J, Schmidt M, et al. Piezo1 and Piezo2 are essential components of distinct mechanically activated cation channels. *Science*. 2010;330:55–60.
128. Nakamichi R, Ma S, Nonoyama T, et al. The mechanosensitive ion channel PIEZO1 is expressed in tendons and regulates physical performance. *Sci Transl Med*. 2022; 14:eabj5557.
129. Solis AG, Bielecki P, Steach HR, et al. Mechanosensation of cyclical force by PIEZO1 is essential for innate immunity. *Nature*. 2019;573:69–74.
130. Marchant CL, Malmi-Kakkada AN, Espina JA, Barriga EH. Cell clusters softening triggers collective cell migration in vivo. *Nat Mater*. 2022;21(11):1314–1323.
131. Agarwal P, Lee HP, Smeriglio P, et al. A dysfunctional TRPV4–GSK3 $\beta$  pathway prevents osteoarthritic chondrocytes from sensing changes in extracellular matrix viscoelasticity. *Nat Biomed Eng*. 2021;5:1472–1484.
132. Goswami R, Arya RK, Sharma S, et al. Mechanosensing by TRPV4 mediates stiffness-induced foreign body response and giant cell formation. *Sci Signal*. 2021; 14:eabd4077.
133. Dutta B, Goswami R, Rahaman SO. TRPV4 plays a role in matrix stiffness-induced macrophage polarization. *Front Immunol*. 2020;11:570195.
134. Nam S, Gupta VK, Lee HP, et al. Cell cycle progression in confining microenvironments is regulated by a growth-responsive TRPV4-PI3K/Akt-p27 Kip1 signaling axis. *Sci Adv*. 2019;5:eaaw6171.
135. Mammoto A, Ingber DE. Cytoskeletal control of growth and cell fate switching. *Curr Opin Cell Biol*. 2009;21:864–870.
136. Hoffman BD, Crocker JC. Cell mechanics: dissecting the physical responses of cells to force. *Annu Rev Biomed Eng*. 2009;11:259–288.
137. Bachmann M, Kukkurainen S, Hytönen VP, Wehrle-Haller B. Cell adhesion by integrins. *Physiol Rev*. 2019;99:1655–1699.
138. Bennett M, Cantini M, Reboud J, Cooper JM, Roca-Cusachs P, Salmeron-Sanchez M. Molecular clutch drives cell response to surface viscosity. *Proc Natl Acad Sci USA*. 2018;115:1192–1197.
139. Hansen LK, Mooney DJ, Vacanti JP, Ingber DE. Integrin binding and cell spreading on extracellular matrix act at different points in the cell cycle to promote hepatocyte growth. *MBoC*. 1994;5:967–975.
140. Dupont S, Morsut L, Aragona M, et al. Role of YAP/TAZ in mechanotransduction. *Nature*. 2011;474:179–183.
141. Panciera T, Azzolin L, Cordenonsi M, Piccolo S. Mechanobiology of YAP and TAZ in physiology and disease. *Nat Rev Mol Cell Biol*. 2017;18:758–770.
142. Moya IM. Hippo–YAP/TAZ signalling in organ regeneration and regenerative medicine. *Nat Rev Mol Cell Biol*. 2019;20(4):211–226.
143. Han YL, Ronceray P, Xu G, et al. Cell contraction induces long-ranged stress stiffening in the extracellular matrix. *Proc Natl Acad Sci U S A*. 2018;115: 4075–4080.
144. Jerrell RJ, Parekh A. Cellular traction stresses mediate extracellular matrix degradation by invadopodia. *Acta Biomater*. 2014;10:1886–1896.
145. Zhao P, Sun T, Lyu C, et al. Scar-degrading endothelial cells as a treatment for advanced liver fibrosis. *Adv Sci*. 2023;10:2203315.
146. Lieber AD, Yehudai-Resheff S, Barnhart EL, Theriot JA, Keren K. Membrane tension in rapidly moving cells is determined by cytoskeletal forces. *Curr Biol*. 2013;23: 1409–1417.